Predicting the morphology of ice particles in deep convection using the super-droplet method

Shin-ichiro Shima (U Hyogo/R-CCS), Yousuke Sato (Hokkaido U/R-CCS), Akihiro Hashimoto (MRI), and Ryohei Misumi (NIED)

Sep 24, 2021

Outline

Summary of SS et al., GMD (2020), 10.5194/gmd-13-4107-2020.

Super-Droplet Method (SDM) is applied to mixed-phase clouds.

Ice morphologies are explicitly predicted.

2D LES of a cumulonimbus is conducted for performance evaluation

Contents

0. SDM (SS et al. 2009)

- A particle-based scheme for cloud micropyhsics
- Super-Droplet represents multiple number of real particles
- **Original Monte Carlo scheme for coalescence**
- **Suitable for detailed cloud microphysics**
- Applicable if particles collide and coalesce repeatedly

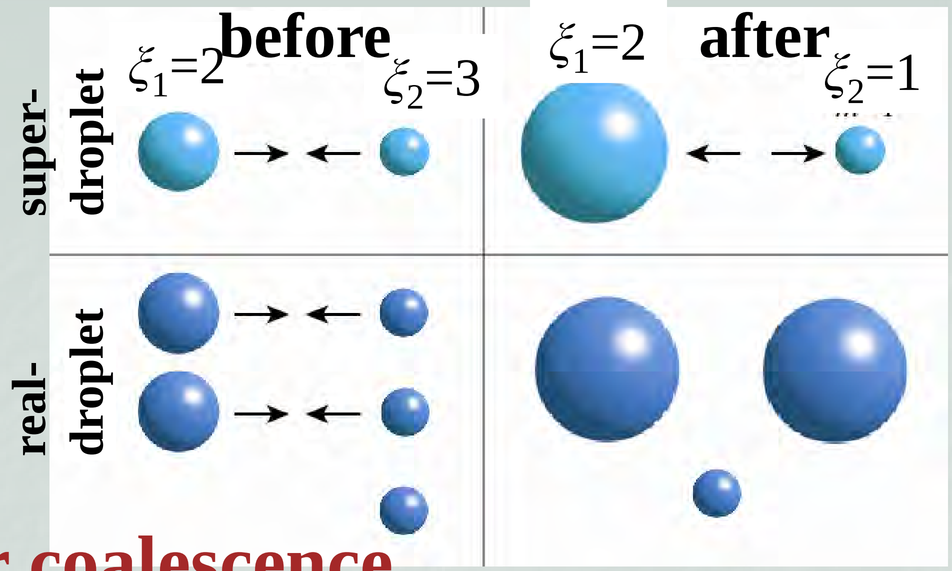

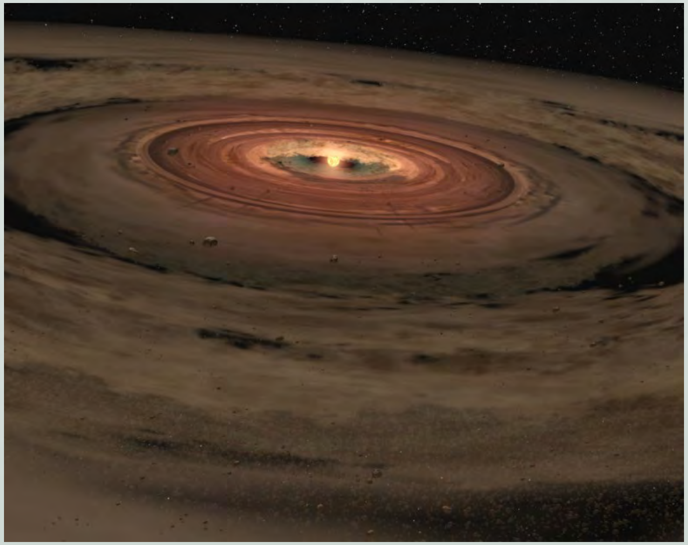

Protoplanetary disk (imaginary. from NASA HP)

Star formation, Spray combustion, bubbles, volcanic fumes, population dynamics etc.

Particle representation in SDM, bin, and bulk

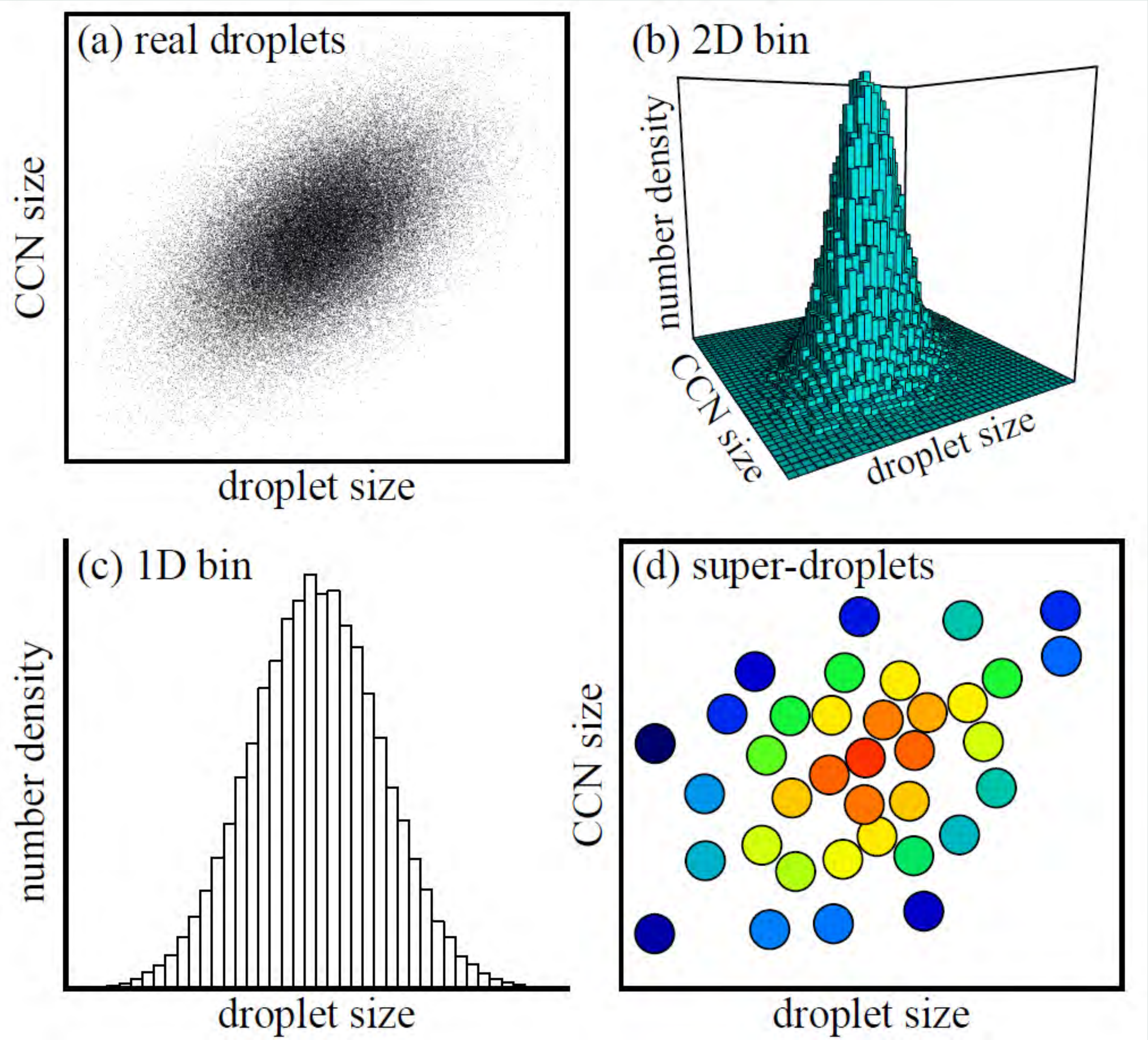

Fig.4 of Grabowski et al. (2019) (created by Shima)

SDM could resolve various issues of bin and bulk (Grabowski et al., 2019)

In bulk models, only the statistical properties (mass, number, etc.) of the particle size dist. are calculated.

For what can we use SDM and other particle-based models?

- Warm clouds: Many studies
  - Cumulus, cumulus congestus, stratocumulus, fog, etc.
- Aerosol processing and aqueous/surface chemistry
  - Jaruga and Pawlowska (2018) reproduced the formation of Hoppel gap from the first princple
- Ice-/mixed-phase clouds
  - Sölch and Kärcher (2010), Brdar and Seifert (2018)
  - **We developed a model that explicitly predict the morphology of ice particles (SS et al., GMD, 2020)**
- Supersaturation fluctuation by SGS turbulence
  - By adding 4 new attributes (S’,U’,V’,W’) (Grabowski and Abade 2017, Abade et al. 2018)
  - By introducing Linear Eddy Model (Hoffman et al., 2018)

1. Cloud Microphysics of Mixed-Phase Clouds

Various ice nucleation pathways

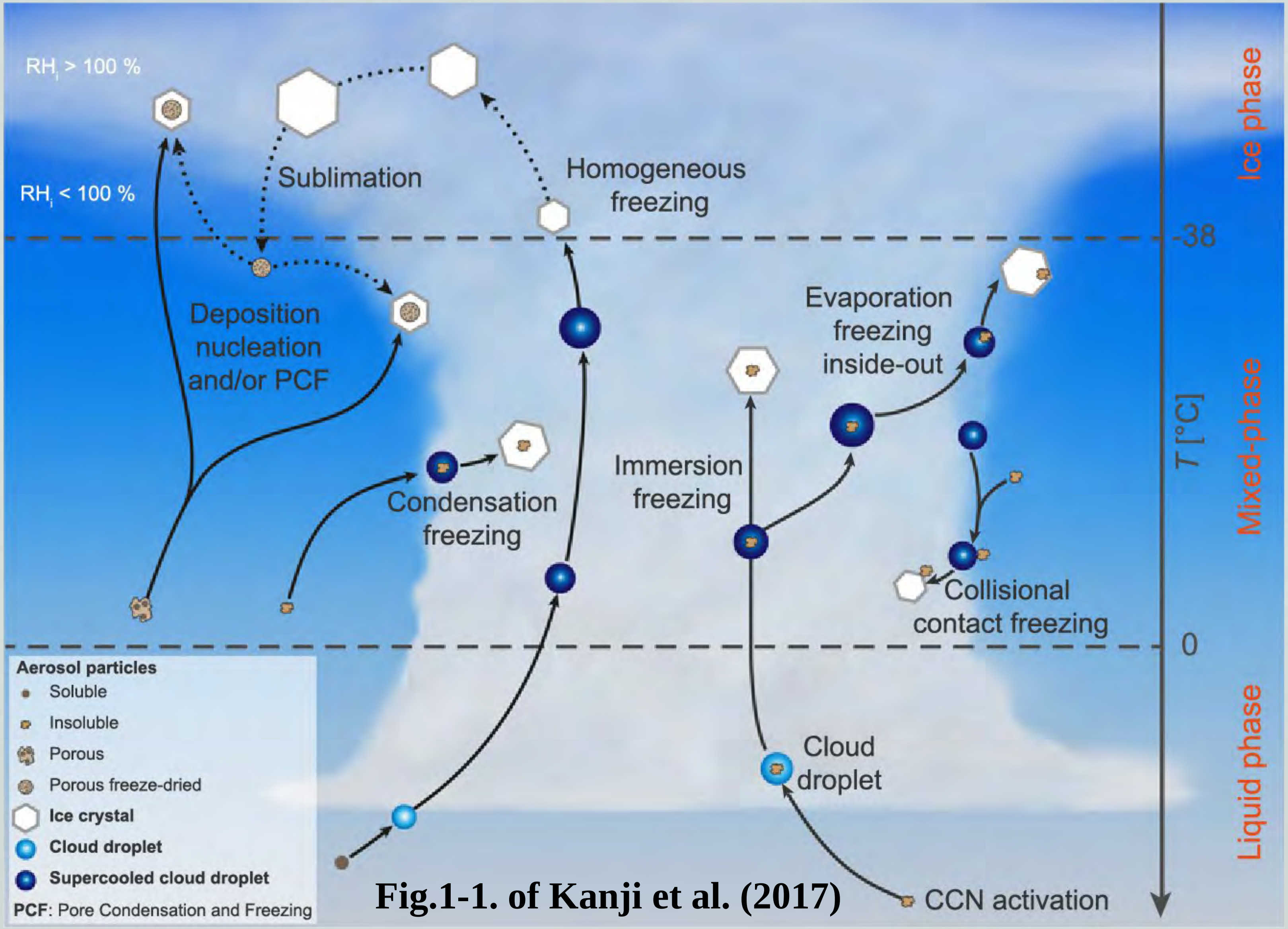

Fig.1-1. of Kanji et al. (2017)

Various other processes

- Freezing
- Melting
- Deposition/sublimation
- Riming (ice-droplet)
- Aggregation (ice-ice)
- Breakup
- etc.

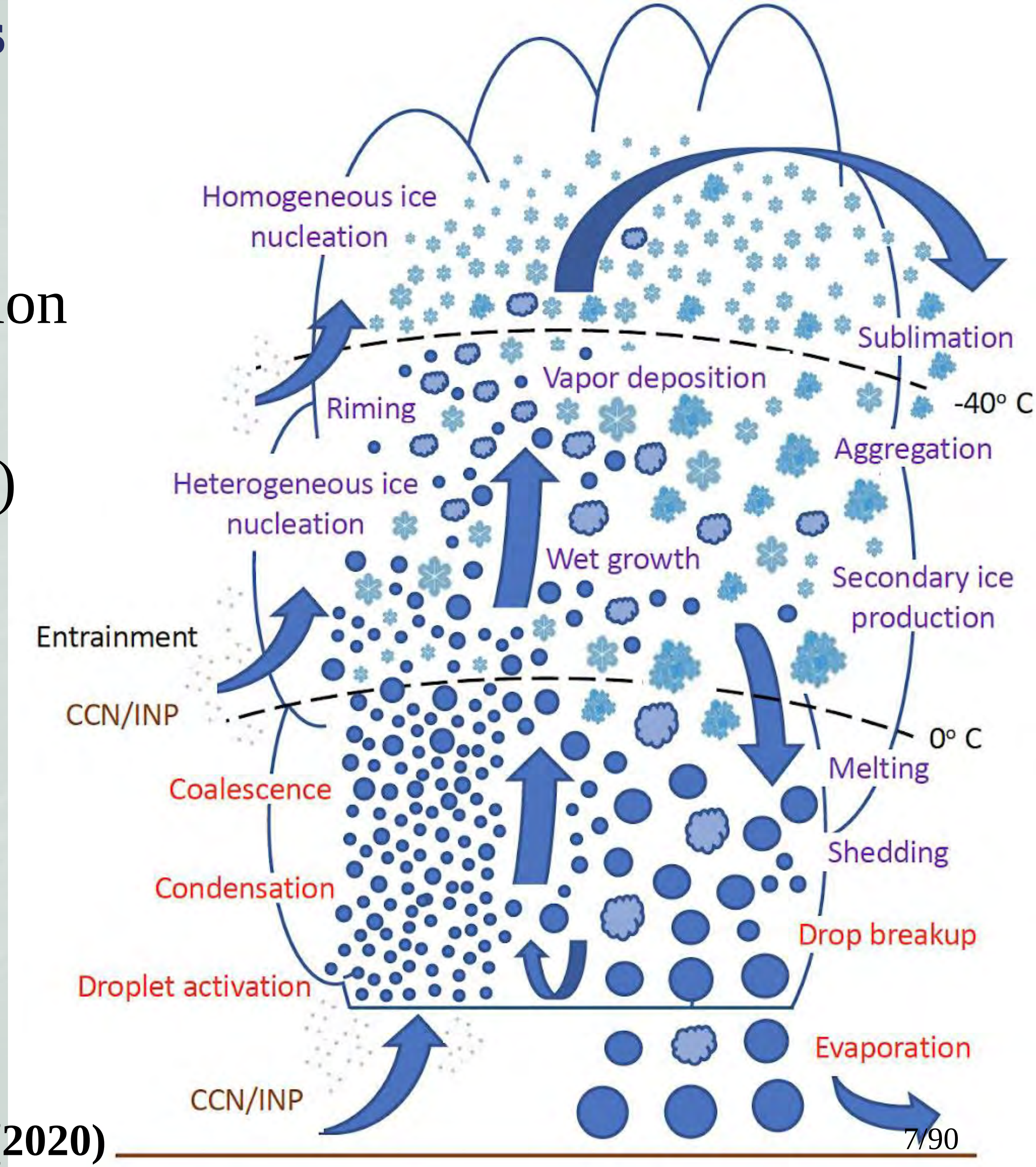

Fig. 1 of Morrison et al. (2020)

Diverse morphology of ice particles

http://www.mri-jma.go.jp/Dep/fo/fo3/araki/snowcrystals.html#sample

photo by K. Araki

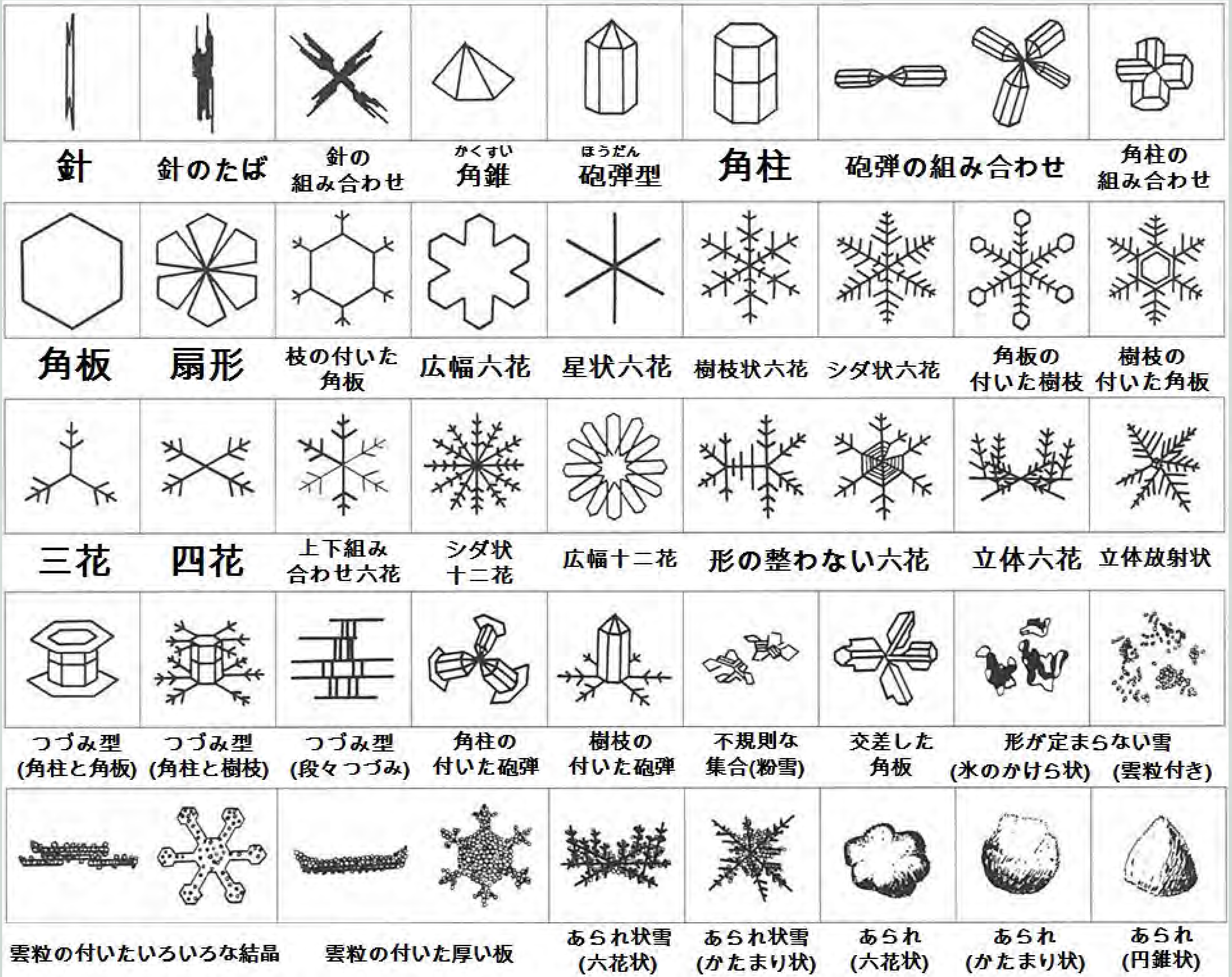

中谷宇吉郎『Snow Crystals』(1954)による

Araki (2014)「雲の中では何が起こっているのか」

2. Strategy to Apply the SDM

Representation of ice particles

Approximate each ice particle by a porous spheroid (Chen and Lamb 1994, Misumi et al. 2010, Jensen and Harrington 2015, etc.)

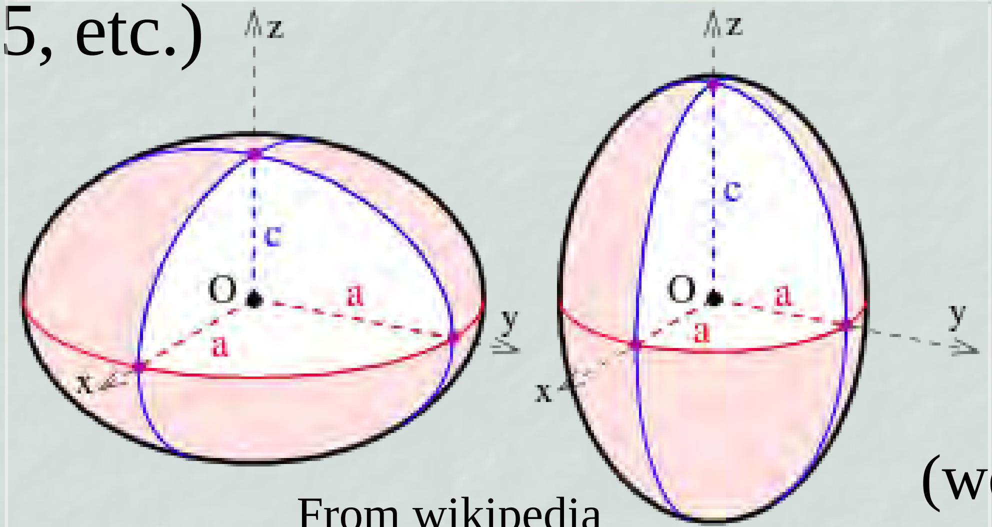

From wikipedia

+ apparent density ρ

(we also track rime mass and number of monomers)

Ice nuclei

Freezing temperature attribute, based on INAS theory

Can account for homogeneous, and condensation/immersion freezing

Cloud microphysics processes considered

- Advection and sedimentation of particles
  - Terminal velocity of droplets
  - **Terminal velocity of ice particles**
- Condensation/evaporation (including CCN act./deact.)
- **Ice particle formation (homogeneous, and condensation/immersion freezing)**
- **Melting**
- **Deposition/sublimation**
- Droplet-droplet collision-coalescence
- **Droplet-ice collision-riming**
- **Ice-ice collision-aggregation**
- (Breakup (collisional/spontaneous)) → **Important but not yet**
- (Collisional/spontaneous breakup of droplets)
- (Collisional fragmentation of ice particles)
- (Rime splintering)
- (Shedding of water droplets from partly melted ice particles)

3. State Variables of Mixed-Phase Clouds

3.1. State Variables for Cloud Micropyhsics

Real particles

"Particles" represent aerosol/cloud/precipitation particles

$\boldsymbol{x}(t)$: position of a particle

$\boldsymbol{a}(t)=\{a^{(1)}(t), a^{(2)}(t), \ldots, a^{(d)}(t)\}$: state of a particle, which is composed of d number of variables, called attributes.

N_r^{wp}: total num of particles accumulated over the whole period

Then, **the state of the cloud microphysical system is determined by**

$$\{\{\boldsymbol{x}_i(t), \boldsymbol{a}_i(t)\}, i = 1, 2, \ldots, N_{\mathrm{r}}^{\mathrm{wp}}\}$$

Particle attributes for mixed-phase clouds

- Mass of soluble substances: m_α^{sol}, α=1, 2,…, N^{sol}
- Mass of insoluble substances: m_β^{ins}, β=1, 2,…, N^{ins}
- Volume equivalent radius of a droplet: r
- **Equatorial radius of an ice particle:** a
- **Polar radius of an ice particle:** c
- **Apparent density of an ice particle:** ρ^{i}
- **Freezing temperature of a particle:** T^{fz}
- **Rime mass:** m_{rime} **(Just for analysis. Not for time evolution)**
- **Number of monomers (primary ice crystal):** n_{mono} **(Just for analysis)**
- Velocity: $\boldsymbol{v}$ (Approximated by theterminal velocity)

Prognostic attributes: $\{r, \{m_\alpha^{\mathrm{sol}}\}, T^{\mathrm{fz}}, a, c, \rho^{\mathrm{i}}\}$

3.2. State Variables for Moist Air Fluid Dynamics

Field variables for moist air

$\boldsymbol{U}=(U,V,W)$: wind velocity

ρ, ρ_d, ρ_v: density of moist air, dry air, and vapor; $\rho := \rho_d+\rho_v$

q_v: specific humidity; $q_v := \rho_v/\rho$

q_d: mass of dry air per unit mass of moist air; $q_d := \rho_d/\rho$

T: temperature

P: pressure

θ: potential temperature of moist air; $\theta := T/\Pi := T/(P/P_0)^{R/c_p}$.

Here, P_0=1000hPa; R_d, R_v, and $R := q_d R_d + q_v R_v$ are the gas constants of dry air, water vapor, and moist air; and c_{pd}, c_{pv}, and $c_p := q_d c_d + q_v c_v$ are the isobaric specific heats of dry air, water vapor, and moist air.

To simplify notation, $\boldsymbol{G} = \{\boldsymbol{U}, \rho, q_v, \theta, P, T\}$.

Prognostic variables for moist air

We solve the time evolution equations of the following, conservative variables: ρ, ρq_{v}, $\rho \boldsymbol{U}$, $\rho\theta$

4. Time Evolution Equation for Mixed-Phase Clouds

4.1. Kinetic Description of Cloud Microphysics

(Real particles)

$$\{\{\boldsymbol{x}_i(t), \boldsymbol{a}_i(t)\}, i = 1, 2, \ldots, N_{\mathrm{r}}^{\mathrm{wp}}\}$$

(Two types of dynamics)

In this section, we introduce the generic form of the time evolution equations of particles with stochastic coalescence

There are two types of dynamics

Individual dynamics

Stochastic collision-coalescence, -riming, and -aggregation

(Spontaneous/collisional breakup is not considered in this study, but important for clouds)

4.1.1. Advection and Sedimentation of Particles

Motion equation

$$\frac{d}{dt}(m_i \boldsymbol{v}_i) = \boldsymbol{F}_i^{\mathrm{drg}} - m_i g \hat{\boldsymbol{z}}, \qquad \frac{d\boldsymbol{x}_i}{dt} = \boldsymbol{v}_i,$$

where F_i^{drg} is the drag force from moist air.

If terminal velocity is reached, the motion eq. becomes,

$$\boldsymbol{v}_i = \boldsymbol{U}_i - \hat{\boldsymbol{z}} v_i^{\infty}, \qquad \frac{d\boldsymbol{x}_i}{dt} = \boldsymbol{v}_i,$$

where $\boldsymbol{U}_i := \boldsymbol{U}(\boldsymbol{x}_i)$ is the ambient wind velocity, and v^{∞} is the terminal velocity, which is a function of attributes $\boldsymbol{a}_i$ and the state of the ambient air $\boldsymbol{G}_i$.

Relaxation time

A few seconds for millimeter-sized droplets (e.g., Fig. 3 of Wang and Pruppacher, 1977)

10^{-5}s for micrometer-sized droplets (e.g., Chen et al., 2018)

4.1.2. Droplet Terminal Velocity

Beard's formula (1976) for droplets (with a limiter)

$$v_i^\infty = v_{\text{Beard}}^\infty(\min(r_i, 3.5\mu\text{m}); \rho_i, P_i, T_i).$$

Original formula is not applicable if r>3.5mm

This can happen because breakup is not considered

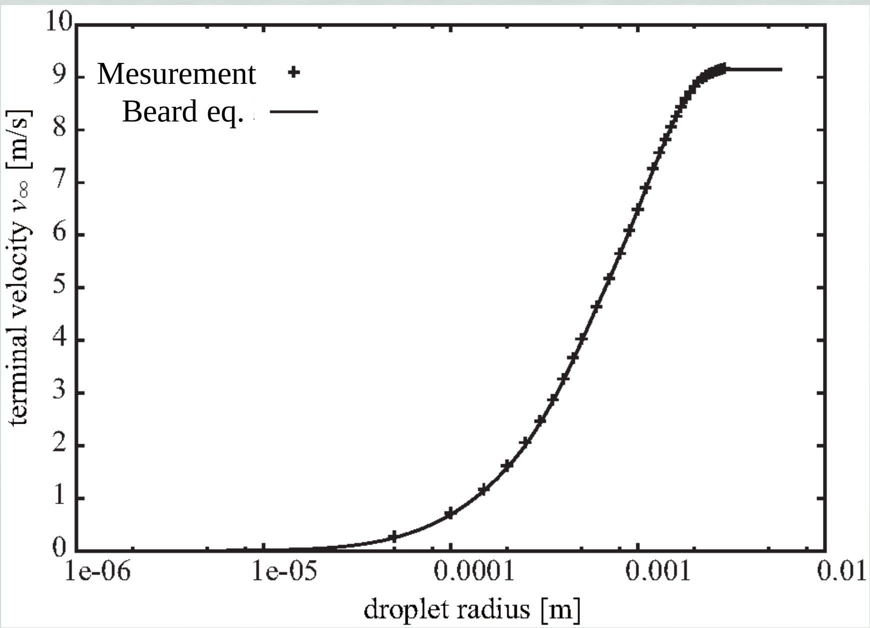

TABLE 1. Formulas for calculating the terminal velocity of cloud drops and raindrops in 3 size ranges.

1. $0.5\ \mu\text{m} \leqslant d_0 \leqslant 19\ \mu\text{m}$

$$V_\infty = C_1 C_{sc} d_0^2$$
$$C_1 = \Delta\rho g/(18\eta),\quad C_{sc} = 1 + 2.51 l/d_0$$
$$l = l_0(\eta/\eta_0)(p_0/p)(T/T_0)^{\frac{1}{2}}$$
$$l_0 = 6.62\times10^{-6}\ \text{cm},\quad p_0 = 1013.25\ \text{mb}$$
$$\eta_0 = 0.0001818\ \text{g cm}^{-1}\ \text{s}^{-1},\quad T_0 = 293.15\ \text{K}$$

2. $19\ \mu\text{m} \leqslant d_0 \leqslant 1.07\ \text{mm}$

$$V_\infty = \eta N_{\text{Re}}/(\rho d_0)$$
$$N_{\text{Re}} = C_{sc}\exp(Y)$$
$$Y = b_0 + b_1 X + \cdots + b_6 X^6$$
$$b_0 = -0.318657\text{E}+1$$
$$\cdot = +0.992696$$
$$\cdot = -0.153193\text{E}-2$$
$$\cdot = -0.987059\text{E}-3$$
$$\cdot = -0.578878\text{E}-3$$
$$\cdot = +0.855176\text{E}-4$$
$$b_6 = -0.327815\text{E}-5$$
$$X = \log_e(N_{\text{Da}})$$
$$N_{\text{Da}} = C_2 d_0^3$$
$$C_2 = 4\rho\Delta\rho g/(3\eta^2)$$

3. $1.07\ \text{mm} \leqslant d_0 \leqslant 7\ \text{mm}$

$$V_\infty = \eta N_{\text{Re}}/(\rho d_0)$$
$$N_{\text{Re}} = N_{\text{P}}^{1/6}\exp(Y)$$
$$N_{\text{P}} = \sigma^3\rho^2/(\eta^4\Delta\rho g)$$
$$Y = b_0 + b_1 X + \cdots b_5 X^5$$
$$b_0 = -0.500015\text{E}+1$$
$$\cdot = +0.523778\text{E}+1$$
$$\cdot = -0.204914\text{E}+1$$
$$\cdot = +0.475294$$
$$\cdot = -0.542819\text{E}-1$$
$$b_5 = +0.238449\text{E}-2$$
$$X = \log_e(\text{Bo}N_{\text{P}}^{1/6})$$
$$\text{Bo} = C_3 d_0^2$$
$$C_3 = 4\Delta\rho g/3\sigma$$

4.1.3. Ice Particle Terminal Velocity

How to evaluate A_i, the actual area size of particle i perpendicular to the fall direction

Let us assume A_i has the following form

$$A_i = \pi a_i \max(a_i, c_i) \underbrace{\left(\rho_i^{\mathrm{i}} / \rho_{\mathrm{true}}^{\mathrm{i}}\right)}_{1-\text{porosity}}{}^{\kappa(\phi_i)}.$$

Let us estimate $k(\varphi_i)$.

For columnar ice crystals (φ_i>>1),

$m_i \propto D_i^{\beta}$, $A_i \propto D_i$, $V_i \propto D_i$, $\rho_i^{\mathrm{i}} = m_i / V_i \propto D_i^{\beta-1}$.

Because of the above relation, $D_i = D_i D_i^{(\beta-1)k}$.

Therefore $k(\varphi_i)=0$, if φ>>1.

For platelike or dendritic ice crystals (φ_i<<1),

$m_i \propto D_i^{\beta}$, $A_i \propto D_i^{\beta}$, $V_i \propto D_i^{2}$, $\rho_i^{\mathrm{i}} = m_i / V_i \propto D_i^{\beta-2}$.

Then, $D_i^{\beta} = D_i^{2} D_i^{(\beta-2)k}$. Thus, $k(\varphi_i)=1$, if φ_i<<1.

… How to evaluate A_i

… Let us estimate $k(\varphi_i)$

For spherical ice particles ($\varphi_i \cong 1$),

$m_i \propto D_i^{\beta}$, $A_i \propto D_i^{\beta/S}$, $V_i \propto D_i^{3}$, $\rho_i^{\mathrm{i}} = m_i/V_i \propto D_i^{\beta-3}$.

Then, $D_i^{\beta/S} = D_i^{2} D_i^{(\beta-3)k}$. Therefore,

$k = (2S-\beta)/(3-\beta)/S$

Snow aggregates of CRYSTAL-FACE obey $\beta=2.22$, $S=1.3$ (Schmitt and Heymsfield (2010))

Therefore, $k=0.375$.

Snow aggregates of ARM (composed of columnar ice) obey $\beta=2.20$, S=1.25 (Schmitt and Heymsfield (2010))

Therefore, $k=0.300$.

Graupels/hails have higher ρ_i^{i}. So, they should be less sensitive to the choice of k.

… How to evaluate *A*

… Let us estimate $k(\varphi)$

All in all, let us estimate the functional form of k as

$$\kappa(\phi_i) = \exp(-\phi_i).$$

A can be evaluated by $A_i = \pi a_i \max\left(a_i, c_i\right) \overbrace{\left(\rho_i^{\mathrm{i}} / \rho_{\mathrm{true}}^{\mathrm{i}}\right)}^{1-\text{porosity}} {}^{\kappa}$

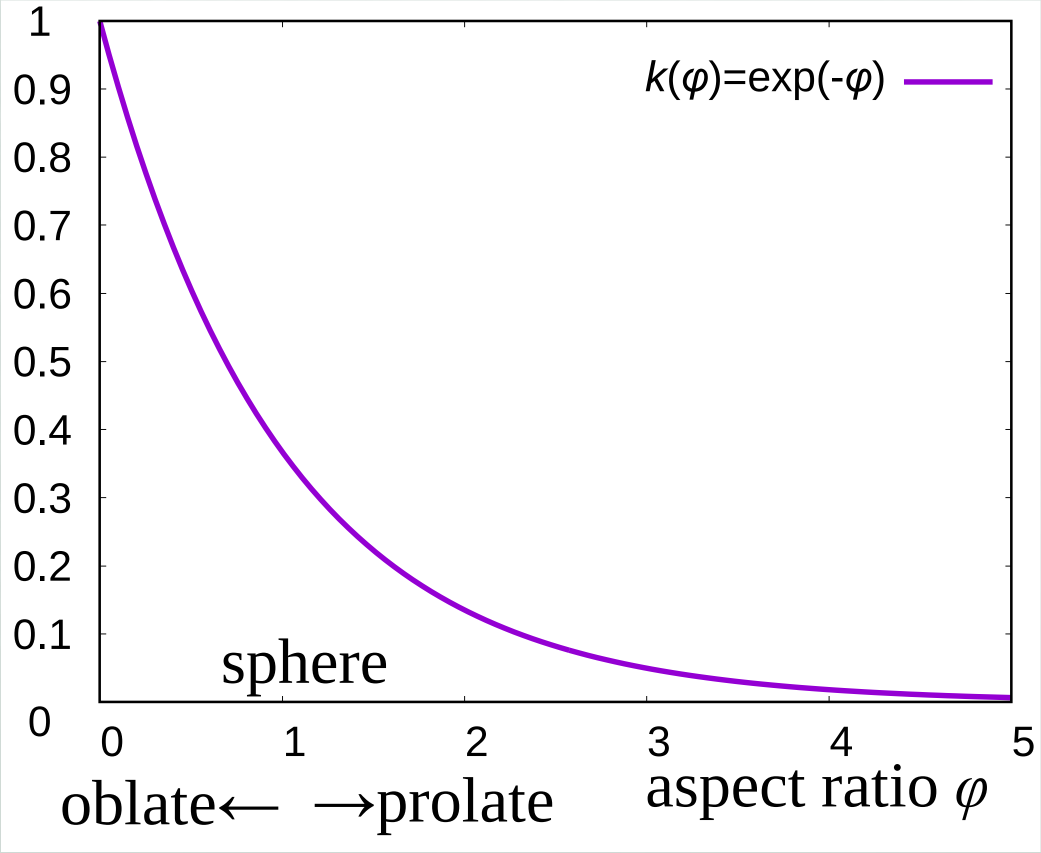

… How to evaluate *A*

Jensen and Harrington (2015) propose

$$A = \pi a \max(a, c)\xi$$

$$\xi = \begin{cases} (1-\phi)\left(\rho^{\mathrm{i}}/\rho_{\mathrm{ice}}\right)+\phi, & \text{for plates (oblate)} \\ 1, & \text{for columns (prolate)} \end{cases}$$

Looks reasonable for lightly rimed particles, but **would be not appropriate for graupels, hails, snow aggregates**

Ice particle terminal velocity formula of Böhm (1989, 1992, 1999)

Applicable for *Re*<5×10^5

$$v^{\infty} = v^{\infty}_{\text{Böhm}}(m_i, \phi_i, d_i, q_i; \rho_i, T_i)$$

Here, $q_i = A_i / (\pi a_i \max(a_i, c_i))$, $d_i = 2a_i$.

Because $q_i \leqq 1$ holds, the formula can be summarized as follows.

The Davies or Best number

$$X = \frac{8 m_i g \rho_i}{\pi \mu^2 \max(\phi_i, 1) q_i^{1/4}},$$

Turbulence correction

$$X' = X \frac{1 + (X/X_0)^2}{1 + 1.6 (X/X_0)^2},$$

Here, $X_0 = 2.8 \times 10^6$ for ice particles

Viscous shape factor

$$k = \min\left\{ \max(0.82 + 0.18\phi_i, 0.85), \left(0.37 + \frac{0.63}{\sqrt{\phi_i}}\right), \frac{1.33}{\max(\log \phi_i, 0) + 1.19} \right\},$$

… Ice particle terminal velocity formula of Böhm

... Summary of the formula

Pressure drag coefficient

$$C_{\mathrm{DP}} = \max\left(0.292k\Gamma, 0.492 - 0.200/\sqrt{\phi_i}\right),$$

where

$$\Gamma = \max\left\{1, \min\left(1.98, 3.76 - 8.41\phi_i + 9.18\phi_i^2 - 3.53\phi_i^3\right)\right\}.$$

Oseen drag coefficient

$$C_{\mathrm{DO}} = 4.5k^2 \max\left(\phi_i, 1\right).$$

Auxiliary parameters

$$\beta = \left[1 + \frac{C_{\mathrm{DP}}}{6k}\left(\frac{X'}{C_{\mathrm{DP}}}\right)^{1/2}\right]^{1/2} - 1,$$

$$\gamma = \frac{C_{\mathrm{DO}} - C_{\mathrm{DP}}}{4C_{\mathrm{DP}}}.$$

… Ice particle terminal velocity formula of Böhm

... Summary of the formula

Reynolds number

$$N_{\mathrm{Re}} = \frac{6k}{C_{\mathrm{DP}}}\beta^2\left[1 + \frac{2\beta e^{-\beta\gamma}}{(2+\beta)(1+\beta)}\right].$$

Here, [] is a matching to low Reynolds number

Finally, terminal velocity can be obtained by

$$v^{\infty}_{\mathrm{B\ddot{o}hm}} = \frac{\mu N_{\mathrm{Re}}}{\rho d_i}.$$

… Ice particle terminal velocity formula of Böhm

Remark

- Brdar and Seifert (2018) is using Khvorostyanov and Curry (2005) (based on Böhm (1989, 1992, 1999)??)
- Maybe we need to check the difference

- Heymsfield and Westbrook (2010) looks simple and accurate, **but only for *Re*<1000.**

4.1.4. Immersion/condensation and homogeneous freezing

These are the dominant mode in mixed-phase clouds

We assume that each particle has its own freezing temperature T_i^{fz}, and the time dependence is ignored. ("singular hypothesis", e.g. Levine (1950))

Droplet i freezes immediately when all these conditions are met:

(1) $e_i > e_s^{\mathrm{w}}(T_i)$: ambient water vapor is supersaturated over liquid water; and,

(2) $T_i < T_i^{\mathrm{fz}}$: ambient temperature is lower than the freezing temperature

T_i^{fz} can be determined by INAS (Ice Nucleation Active Site) density of the insoluble component

If no INAS appears until −38°C, we set $T_i^{\mathrm{fz}} = -38$°C (homogeneous freezing)

When a coalescence occurs, we assume that the new T^{fz} is given by $\max(T_j^{\mathrm{fz}}, T_k^{\mathrm{fz}})$, i.e., the higher of the two.

INAS density of Niemand et al. (2012)

A parameterization of INAS of mineral dust particles for condensation/immersion freezing mode.

From Eq.(5) of their paper, for $-12℃ > T \geqq -36℃$

$$n_s(T) = 1\mathrm{m}^{-2}\exp[-0.517\mathrm{K}^{-1}(T - T_0) + 8.934]$$
$$=: a_0 \exp[-a_1(T - T_0) + a_2].$$

Based on the discussion of Niedermeier (2015), let's assume

$$n_s(T) \begin{cases} 0, & T \geq -12^\circ\mathrm{C}, \\ n_s(-36^\circ\mathrm{C}), & -36^\circ\mathrm{C} > T \geq -38^\circ\mathrm{C}. \end{cases}$$

Freezing temperature and INAS

Consider a mineral dust with a surface area of A

Then, the probability that the freezing temperature $T^{(f)}$ is larger than T becomes,

$$P(T^{(f)} \geq T) = 1 - e^{-\Lambda(T)}, \quad \Lambda(T) = A n_s(T).$$

Then, the probability density becomes

$$\begin{aligned} p(T) &= -dP(T(f) \geq T)/dT \\ &= a_1 A n_s(T) e^{-A n_s(T)}. \end{aligned}$$

Freezing temperature distribution of mineral dust based on Niemand et al. (2012)'s formula

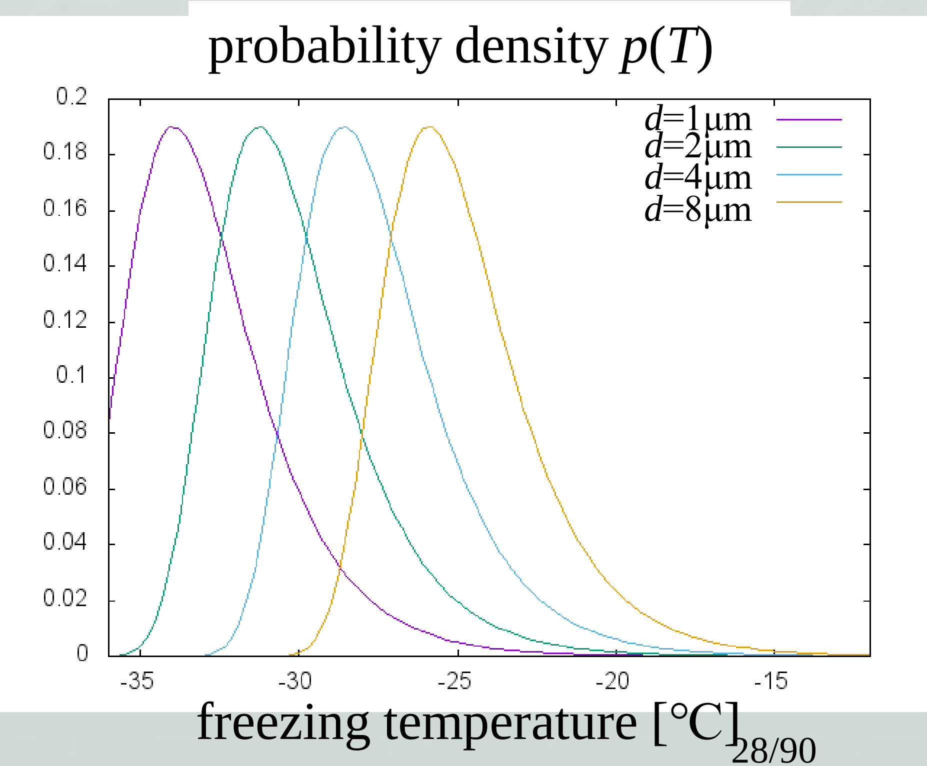

4.1.5. Melting

When $T_i > 0°C$, we consider that melting occurs immediately.

4.1.6. Condensation and Evaporation

Overview of the phenomenon

When supersaturated, water vapor condensates to droplets

When unsaturated, water vapor evaporates from droplets

Here, the effective saturation vapor pressure is affected by the curvature effect and dissolution effect of aerosols

Equation of growth by condensation/evaporation

If the diffusion of vapor around the droplet is quasi-steady,

$$\frac{dm_i}{dt} = 4\pi r_i D_{\mathrm{v}} (\rho_{\mathrm{v}i} - \rho_{\mathrm{v}i}^{\mathrm{sfc}}).$$

Here, D_{v} is water vapor's diffusivity in air, $\rho_{\mathrm{v}i} := \rho_{\mathrm{v}}(\boldsymbol{x}_i)$ is the ambient water vapor density, and $\rho_{\mathrm{v}i}{}^{\mathrm{sfc}}$ is the water vapor density at the surface of the droplet.

... Equation of growth by condensation/evaporation

However, ρ_{vi}^{sfc} is unknown bcz condensation/evaporation changes the droplet temperature

If we further assume that thermal diffusion is also quasi-steady, and that the surface temperature T_i^{sfc} and ambient temperature T_i are close to each other, the eq reduces to

$$r_i \frac{dr_i}{dt} = \frac{1}{\rho^{\mathrm{w}}(F_{\mathrm{k}}^{\mathrm{w}} + F_{\mathrm{d}}^{\mathrm{w}})} \left\{ S_i^{\mathrm{w}} - \frac{e_{\mathrm{s}i}^{\mathrm{w,eff}}(T_i)}{e_{\mathrm{s}}^{\mathrm{w}}(T_i)} \right\},$$

where $S^{\mathrm{w}}_i := e_i/e_{\mathrm{s}}^{\mathrm{w}}(T_i)$ is the ambient saturation ratio over liquid water,

$$F_{\mathrm{k}}^{\mathrm{w}} = \left(\frac{L_{\mathrm{v}}}{R_{\mathrm{v}} T_i} - 1 \right) \frac{L_{\mathrm{v}}}{k T_i}, \quad F_{\mathrm{d}}^{\mathrm{w}} = \frac{R_{\mathrm{v}} T_i}{D_{\mathrm{v}} e_{\mathrm{s}}^{\mathrm{w}}(T_i)},$$

L_{v} is the latent heat of vaporization, k is the thermal conductivity of moist air, and $e_{\mathrm{s}i}^{\mathrm{w,eff}}$ is the effective saturation vapor pressure regarding droplet's surface.

... Equation of growth by condensation/evaporation

Köhler curve (1936) gives an approximate formula of $e_{si}^{\mathrm{w,eff}}$

$$\frac{e_{\mathrm{s}i}^{\mathrm{w,eff}}(T_i)}{e_{\mathrm{s}}^{\mathrm{w}}(T_i)} = 1 + \frac{a(T_i)}{r_i} - \frac{b\left(\left\{m_{\alpha i}^{\mathrm{sol}}\right\}\right)}{r_i^3},$$

where $a \approx 3.3\mathrm{x}10^{-5}$ cm K/T_i, $b \approx 4.3$ cm$^3 \sum_\alpha I_\alpha\, m_{\alpha i}^{\mathrm{sol}} / M_\alpha^{\mathrm{sol}}$, I_α is the van't Hoff factor, which represents the degree of ionic dissociation, and M_α^{sol} is the molecular weight of the solute α.

The second and third terms of Köhler curve account for the curvature and solute effects, respectively.

Shape of Köhler curves

Köhler curve for a droplet containing ammonium sulfate 10^{-16}g at 293K is

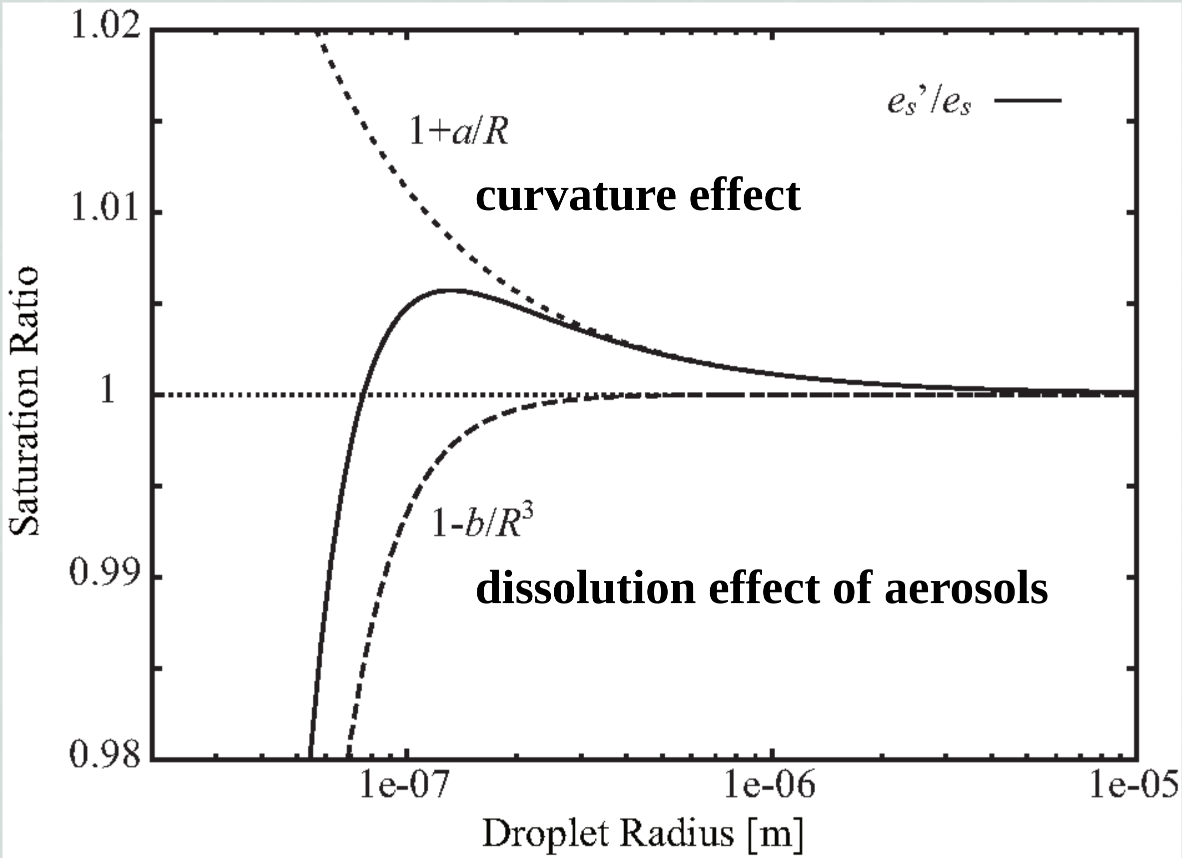

Cloud droplets won't be created until supersaturation exceeds the critical value. When unsaturated, droplet becomes very small but does not vanish.

4.1.7. Deposition and Sublimation

Primary/Secondary growth habit

Strong dependence on temperature (primary habit), and, to a lesser extent, on supersaturation (secondary habit).

We use the model of Chen and Lamb (1994) with various modifications

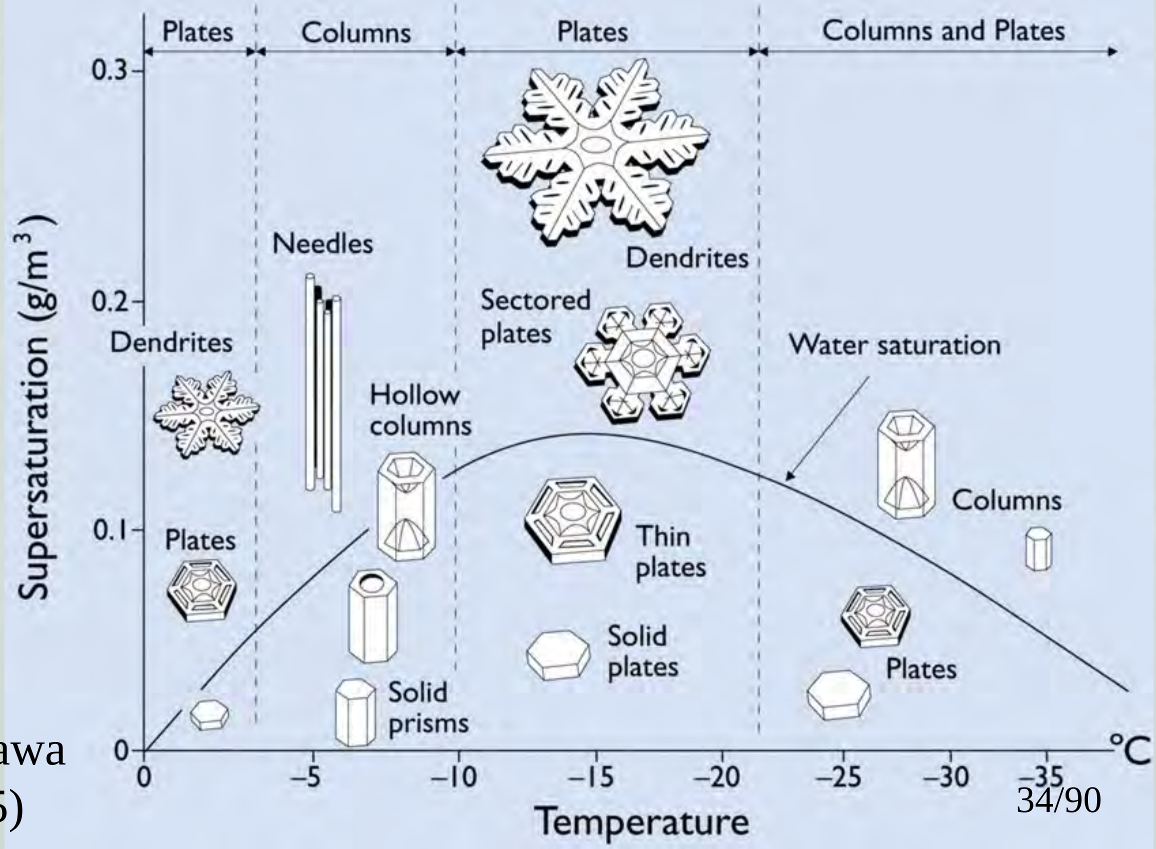

Variant of Nakaya-Kobayashi-Furukawa diagram (Fig. 2 of Libbrecht, 2005)

Time evolution eqs. of deposition/sublimation

Mass growth eq.

$$\frac{dm_i}{dt} = 4\pi C D_{\rm v}(\rho_{{\rm v}i} - \rho_{{\rm v}i}^{\rm sfc})\bar{f}_{\rm vnt} = 4\pi C \frac{S_i^{\rm i} - 1}{F_{\rm k}^{\rm i} + F_{\rm d}^{\rm i}} \bar{f}_{\rm vnt}.$$

Here, $S^{\rm i}_i := e_i / e_{\rm s}^{\rm i}(T_i)$ is the ambient saturation ratio over ice,

$$F_{\rm k}^{\rm i} = \left(\frac{L_{\rm s}}{R_{\rm v} T_i} - 1\right)\frac{L_{\rm s}}{kT_i}, \quad F_{\rm d}^{\rm i} = \frac{R_{\rm v} T_i}{D_{\rm v} e_{\rm s}^{\rm i}(T_i)},$$

C is the electric capacitance of ice, which we approximate by the capacitance of the spheroid $C(a_i,c_i)$.

$\bar{f}_{\rm vnt} = b_1 + b_2 X^{\gamma}, \quad X = N_{\rm Sc}^{1/3}(N_{{\rm Re}i}^{\rm i})^{1/2}$, is the particle-averaged ventilation coefficient.

We impose a limiter to dm_i and prohibit complete sublimation (a crude model of pre-activation)

$$dm_i = \max(dm_i, m_{\rm min}^{\rm i} - m_i).$$

... Time evolution eqs. of deposition/sublimation

Axis growth ratio (primary habit)

$$\frac{dc_i}{da_i} = \Gamma(T_i) f_{\mathrm{vnt}} \frac{c_i}{a_i} =: \Gamma^* \frac{c_i}{a_i}.$$

Inherent growth ratio $\Gamma(T)$ represents the lateral redistribution of vapor on ice surface through kinetic processes.

For deposition (dm_i>0), we use the empirical form of Chen and Lamb (1994) (next page), but set

$$\Gamma(T) = 1 \text{ for } D < 10\,\mu\mathrm{m},$$

$$\Gamma(T) = \Gamma(-30\,^\circ\mathrm{C}) \approx 1.28, \quad \text{for } T < -30\,^\circ\mathrm{C}.$$

For sublimation,

$$\Gamma(T_i) = 1, \quad \text{for } dm_i < 0 \text{ (sublimation)},$$

... Time evolution eqs. of deposition/sublimation

... Axis growth ratio (primary habit)

Inherent growth ratio Γ(*T*) of Chen and Lamb (1994)

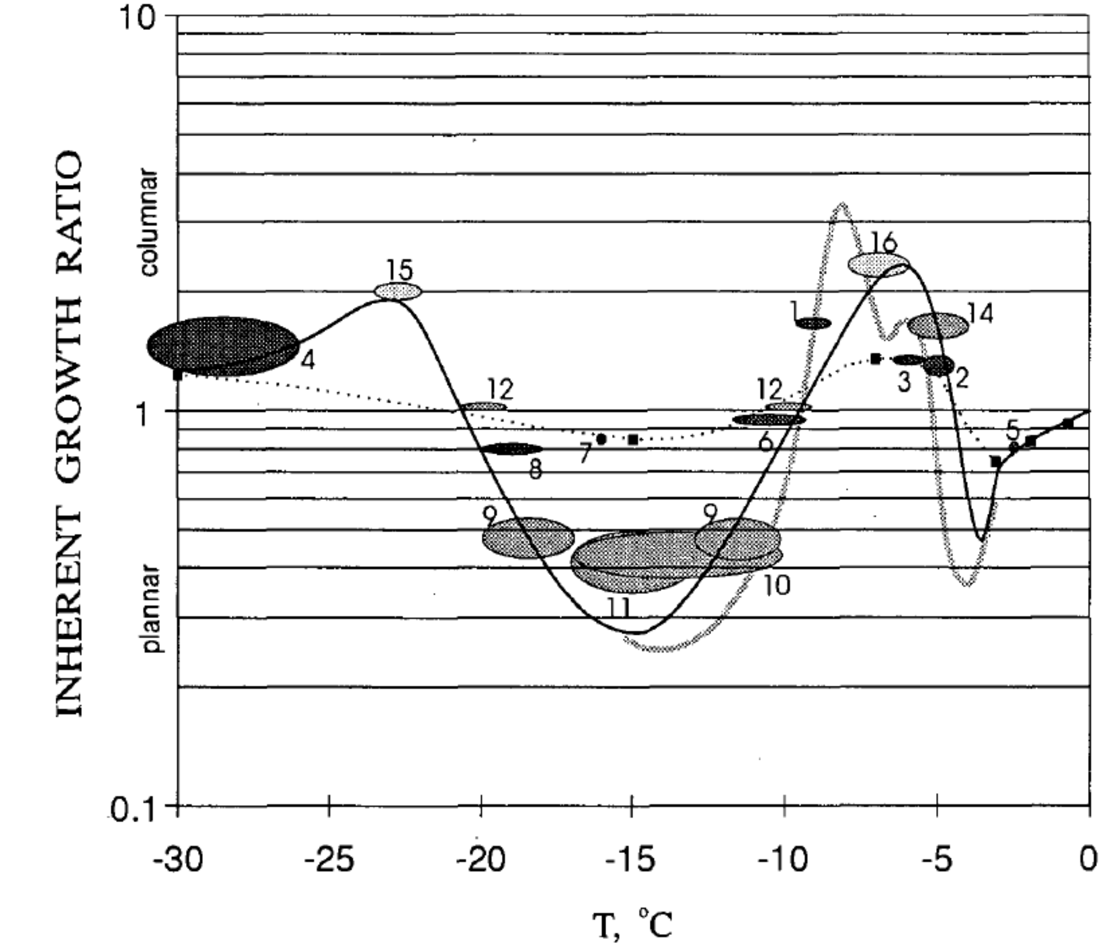

FIG. 3. Comparisons between the experimental and observational values of the inherent growth ratio. The thick line is from Lamb and Scott (1972); dotted line is from Sei and Gonda (1989) with actual data points denoted as filled squares. The shaded ellipses 1 to 8 are from Ono (1970), 9 to 14 from Auer and Veal (1970), 15 from Heymsfield and Knollenberg (1972), and 16 from Jayaweera and Ohtake (1974). The thin solid line is the best-fit values proposed in this study.

Adopted from
Chen and Lamb (1994)

... Time evolution eqs. of deposition/sublimation

... Axis growth ratio (primary habit)

f_{vnt} is the ventilation effect for primary growth habit.

Chen and Lamb (1994) derived

$$f_{\mathrm{vnt}} = \frac{b_1 + b_2 X^{\gamma} \left(c_i/C\right)^{1/2}}{b_1 + b_2 X^{\gamma} \left(a_i/C\right)^{1/2}}.$$

To prohibit the creation of too slender ice particle, we also impose a limiter to Γ*

$$\Gamma^* = \Gamma f_{\mathrm{vnt}} = 1 \quad \text{for } dm_i \geq 0 \ \wedge \ \phi_i > 40.$$

Change in particle volume (secondary habit)

For deposition, $dV_i = \dfrac{dm_i}{\rho_{\mathrm{dep}}}$,

$$\rho_{\mathrm{dep}} = \begin{cases} \rho^{\mathrm{i}}_{\mathrm{true}}, & \text{for } \Gamma(T_i) < 1 \ \wedge \ a_i < 100\,\mu\mathrm{m}; \\ \rho^{\mathrm{CL94}}_{\mathrm{dep}}, & \text{otherwise.} \end{cases}$$

... Time evolution eqs. of deposition/sublimation

... Change in particle volume (secondary habit)

$$\rho_{\mathrm{dep}}^{\mathrm{CL94}} = \rho_{\mathrm{true}}^{\mathrm{i}} \exp\left[-\frac{3\max((\Delta\rho_i)^{\downarrow} - 0.05\,\mathrm{g\,m^{-3}}, 0)}{\Gamma(T_i)\,\mathrm{g\,m^{-3}}}\right],$$

$$(\Delta\rho_i)^{\downarrow} = \frac{\min\left(S_i^{\mathrm{i}}, e_{\mathrm{s}}^{\mathrm{w}}(T_i)/e_{\mathrm{s}}^{\mathrm{i}}(T_i)\right) - 1}{D_{\mathrm{v}}(F_{\mathrm{k}}^{\mathrm{i}} + F_{\mathrm{d}}^{\mathrm{i}})}.$$

For sublimation, $dV_i = \dfrac{dm_i}{\rho_{\mathrm{sbl}}}, \quad \rho_{\mathrm{sbl}} = \rho_i^{\mathrm{i}}.$

Above model could create a very small planar/columnar ice through sublimation. We reset it to spherical if the minor axis becomes <1μm.

Change of rime mass fraction

$$m_i^{\mathrm{rime}}(t+dt) = \begin{cases} m_i^{\mathrm{rime}}, & \text{for } dm_i \geq 0; \\ m_i^{\mathrm{rime}} \dfrac{m_i + dm_i}{m_i}, & \text{for } dm_i < 0. \end{cases}$$

4.1.8. Stochastic Description of Coalescence/Riming/Aggregation

Assuming that the particles are well mixed by turbulence, we regard coalescence/riming/aggregation is a stochastic event

$$P_{jk} = K(\boldsymbol{a}_j, \boldsymbol{a}_k; \boldsymbol{G}) \frac{dt}{\Delta V},$$

$$= \text{probability that particles } j \text{ and } k \text{ inside a small region } \Delta V \text{ will collide and coalesce in a short time interval } (t, t+dt).$$

All the pairs (j,k) inside ΔV have a possibility to coalesce

$P_{jk} \propto dt$ because Poisson process is assumed

$P_{jk} \propto 1/\Delta V$ because particles are well mixed. (If $\Delta V \rightarrow 2\Delta V$, collision candidates for j will be doubled, hence, $P_{jk} \rightarrow P_{jk}/2$)

For riming and aggregation, we also need outcome model.

4.1.9. Coalescence Between Two Droplets

Coalescence of particles by the gravitational settling

Bigger particles sweep smaller particles because of the difference of their terminal velocities

Collision-coalescence probability

Consider two droplets *j* and *k* in a volume ΔV

2 particles sweep the volume $\pi(R_j+R_k)^2|\mathbf{v}_j-\mathbf{v}_k|dt$ during a small time interval $(t, t+dt)$

If ΔV is small enough, particles are well mixed by the atmospheric turbulence

Thus, the probability that the coalescence occurs is the ratio of sweep volume and ΔV:

$$P_{jk} = \pi(r_j + r_k)^2|v_j^\infty - v_k^\infty|dt/\Delta V$$

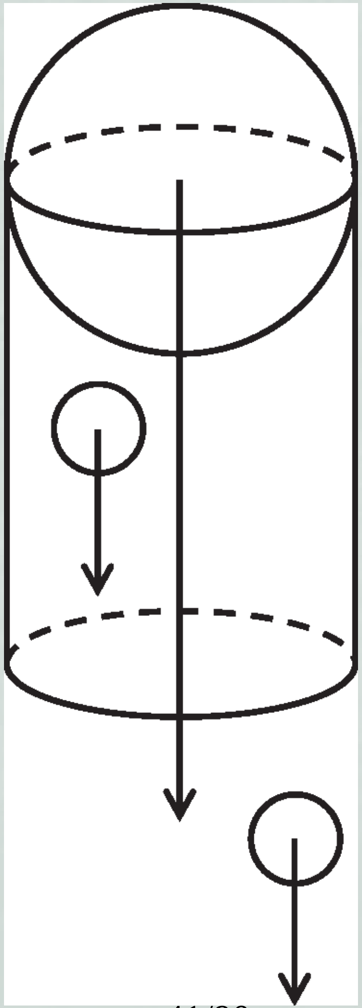

... Collision-coalescence probability

However, this evaluation is not accurate enough.

Small droplet could swept aside, or bounce.

A droplet could collide on the downstream side of a similarly sized droplet. (known as wake capture)

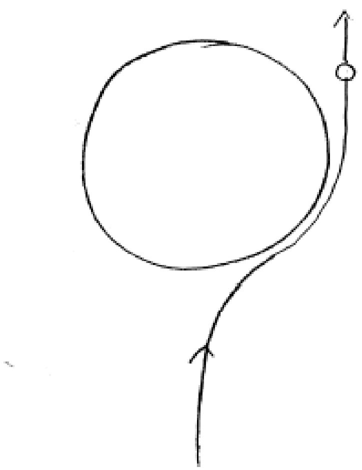

swept aside along the flow

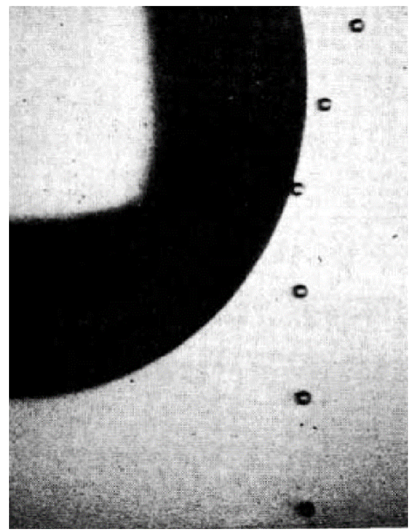

bounce on the surface

collision and bounce of small droplet (35μm in radius) and large droplet (1.75mm in radius). (adapted from Whelpdale and List, 1971)

Collection efficiency $E_{\mathrm{coal}}(r_j, r_k)$ considers these effects

$$P_{jk} = E_{\mathrm{coal}}(r_j, r_k)\pi(r_j + r_k)^2 |v_j^\infty - v_k^\infty| dt/\Delta V$$

... Collision-coalescence probability

- Contour plot of P_{jk} as a function of R_j and R_k
  - E_{coal} in Seeßelberg et al. (1996), which is a compilation of Davis(1972), Jonas(1972), Hall(1980), Lin and Lee (1975). ΔV=1cm^3, Δt=1s, 101.3kPa, 20°C.
- Same size droplets won't coalesce
- Small droplets seldom coalesce
  - Droplets of r>15μm are necessary for rain initiation

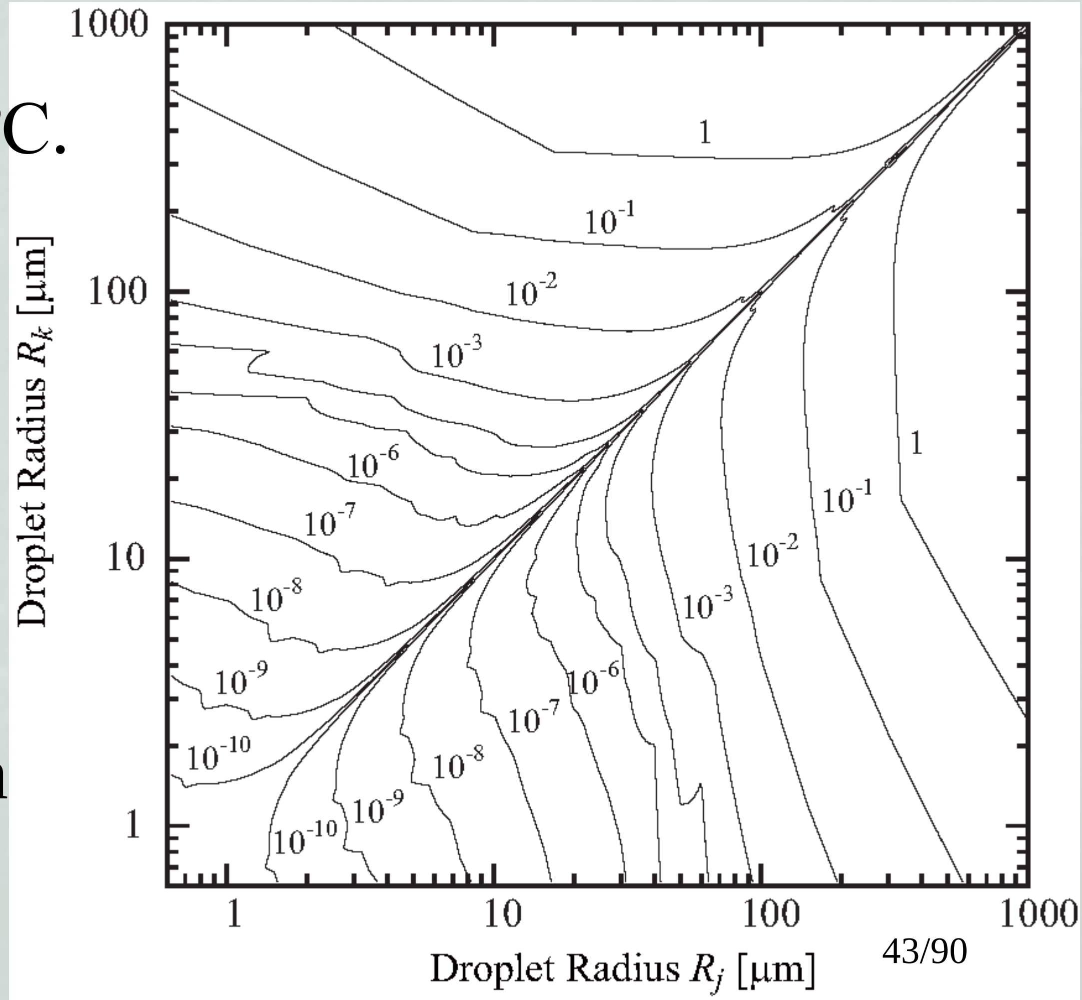

4.1.10. Riming Between an Ice Particle and a Droplet

Not only the collection of small droplets by a large ice, but also the collection of small ice by a large droplets.

Collision-riming kernel

Consider an ice particle j and a droplet k in a volume ΔV

Collision-riming kernel: $K_{\mathrm{rime}} = E_{\mathrm{rime}} A_{\mathrm{g}} |v_j^\infty - v_k^\infty|.$

We approximate the geometric cross sectional area A_{g} by

$$A_{\mathrm{g}} = \pi(a_j + r_k)\{\max(a_j, c_j) + r_k\} - (A_j^{\mathrm{ce}} - A_j).$$

For the collision-riming collection efficiency E_{rime}, we combine the formulas of Beard and Grover (1974) and Erfani and Mitchell (2017).

If $v_j^\infty < v_k^\infty$, droplet k is the collector and adopt BG74:

$$E_{\mathrm{rime}} = E_{\mathrm{BG74}}(p^{\mathrm{i/w}}, N_{\mathrm{Re}k}^{\mathrm{w}}, N_{\mathrm{St}}^{\mathrm{i/w}}), \quad p^{\mathrm{i/w}} := r_j^{\mathrm{i}}/r_k.$$

... Collision-riming kernel

... collection efficiency E_{rime}

If $v_j^{\infty} \geq v_k^{\infty}$, ice j is the collector

For spherical ice, use E_{BG74} again but $N_{\mathrm{St}}^{\mathrm{i/w}} \to N_{\mathrm{mFr}}$.

For columnar and planar ice, $E_{\mathrm{EM17}}^{\mathrm{clm}}$ and $E_{\mathrm{EM17}}^{\mathrm{pln}}$.

For intermediate case, the above are combined by the weight of aspect ratio ϕ_j:

For $\phi_j < 1$ (planar)

$$E_{\mathrm{rime}} = \phi_j E_{\mathrm{BG74}}(p^{\mathrm{w/i}}, N_{\mathrm{Re}j}^{\mathrm{i}}, N_{\mathrm{mFr}}) + (1-\phi_j) E_{\mathrm{EM17}}^{\mathrm{pln}}(N_{\mathrm{Re}j}^{\mathrm{i}}, N_{\mathrm{mFr}}).$$

For $\phi_j \geq 1$ (columnar)

$$E_{\mathrm{rime}} = \frac{1}{\phi_j} E_{\mathrm{BG74}}(p^{\mathrm{w/i}}, N_{\mathrm{Re}j}^{\mathrm{i}}, N_{\mathrm{mFr}}) + \left(1 - \frac{1}{\phi_j}\right) E_{\mathrm{EM17}}^{\mathrm{clm}}(N_{\mathrm{Re}j}^{\mathrm{clm}}, N_{\mathrm{mFr}}).$$

Here, $p^{\mathrm{w/i}} := 1/p^{\mathrm{i/w}} = r_k / r_j^{\mathrm{i}}$

Outcome of riming: $(a_j, c_j, \rho^i_j) + r_k \longrightarrow (a_j', c_j', \rho^i_j{}')$

If $r_k > \max(a_j, c_j)$, we assume the resultant ice is spherical, $a_j' = c_j'$, with the true ice density $\rho_j' = \rho^i_{\text{true}}$

Otherwise,

for $\phi_j \le 0.8$ or $1.25 < \phi_j$, preserve the maximum dimension (filling-in simplification);

for $0.8 < \phi_j \le 1.25$, preserve the minor dimension (graupel tumbling);

if the frozen droplet is bigger than the ice, we preserve $r_k(\rho^{\mathrm{w}}/\rho_{\text{rime}})^{1/3}$.

ρ_{rime} represents the frozen droplet's apparent density.

We use the formula of Heymsfield and Pflaum (1985) with some modifications:

... Outcome of riming: $(a_j, c_j, \rho^i_j) + r_k \longrightarrow (a_j', c_j', \rho^i_j{}')$

... ρ_{rime} of Heymsfield and Pflaum (1985)

$$\rho_{\mathrm{rime}} = \max\{\min\{\rho^{\mathrm{HP85}}_{\mathrm{rime}}(Y), 0.91\,\mathrm{g\,cm^{-3}}\}, 0.1\,\mathrm{g\,cm^{-3}}\},$$

$$\rho^{\mathrm{HP85}}_{\mathrm{rime}}(Y) = \begin{cases} (\mathrm{g\,cm^{-3}})\exp\left(B_2 + B_3 Y^{\downarrow} + B_4 Y^{\downarrow 2} + B_5 Y^{\downarrow 3}\right), & \\ & \text{for } T^{\mathrm{sfc}}_j > -5^\circ\mathrm{C} \wedge Y > 1.6; \\ A Y^{B_1}, & \text{otherwise}, \end{cases}$$

$$Y := \frac{-r_k v_{\mathrm{imp}} / T^{\mathrm{sfc}}_j}{\mu\mathrm{m\,ms^{-1}}/^\circ\mathrm{C}},$$

$$Y^{\downarrow} = \min(Y, 3.5).$$

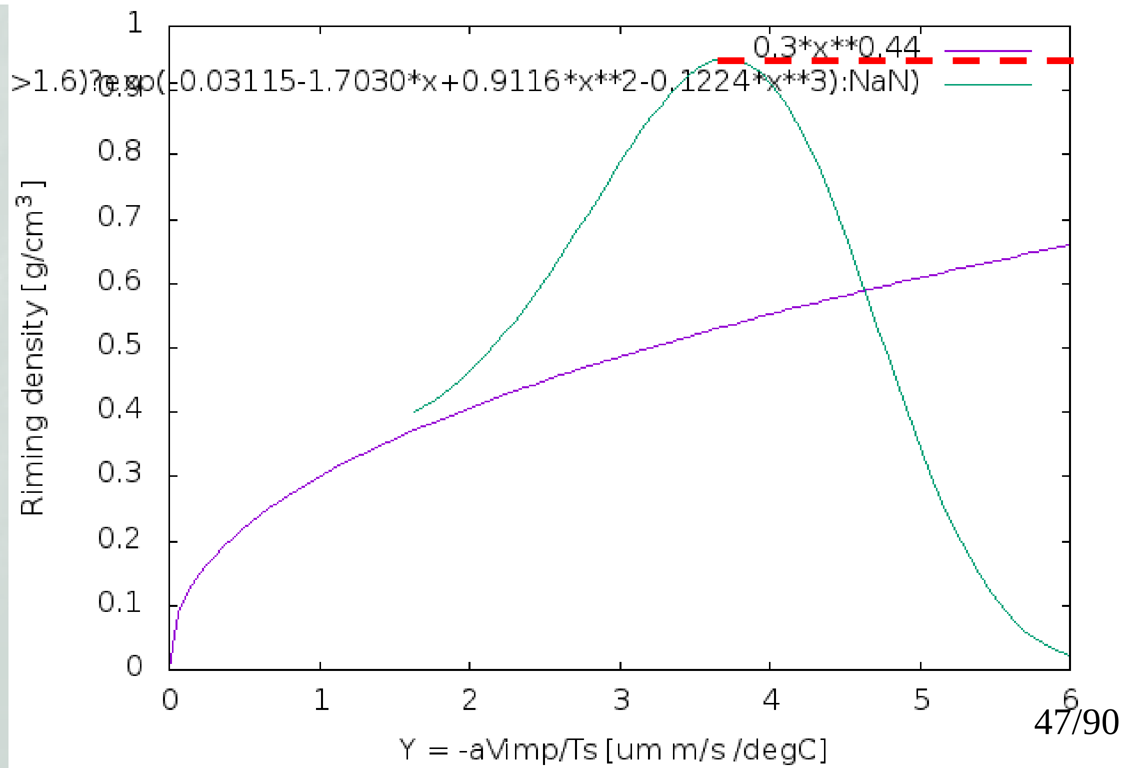

4.1.11. Aggregation Between Two Ice Particles

Collision-aggregation kernel

Collision-aggregation kernel:

$$K_{\mathrm{agg}} = E_{\mathrm{agg}} \left(A_j^{\frac{1}{2}} + A_k^{\frac{1}{2}} \right)^2 \left| v_j^\infty - v_k^\infty \right|,$$

Geometric cross section is evaluated by the projected area (Connolly et al., 2012)

E_{agg}=0.1 is assumed for collision-aggregation collection efficiency (Morrison and Grabowski, 2012; Field et al., 2006).

Outcome of aggregation: $(a_j, c_j, \rho^{\mathrm{i}}_j) + (a_k, c_k, \rho^{\mathrm{i}}_k) \longrightarrow (a_j', c_j', \rho^{\mathrm{i}}_j{}')$

Existing procedures produce too light ice particles

We developed an intuitive model to fix this issue

We assume only the minor dimension grows

If the volume weighted average density

$$\bar{\rho}^{\mathrm{i}}_{jk} = (m_j + m_k)/(V_j + V_k)$$

is closer to the true density of ice $\rho^{\mathrm{i}}_{\mathrm{true}}$, we assume that two particles aggregate without changing their shape.

If $\overline{\rho}^{\mathrm{i}}_{jk}$ is small (fluffy snow flakes), we assume that compaction of aggregate through restructuring occurs.

We assume there is a limiting value of the apparent density, $\rho^{\mathrm{i}}_{\mathrm{crt}} = 10\,\mathrm{kg\,m^{-3}}$.

… Outcome of aggregation: $(a_j, c_j, \rho^{\mathrm{i}}_j) + (a_k, c_k, \rho^{\mathrm{i}}_k) \rightarrow (a_j', c_j', \rho^{\mathrm{i}}_j{}')$

… Our model

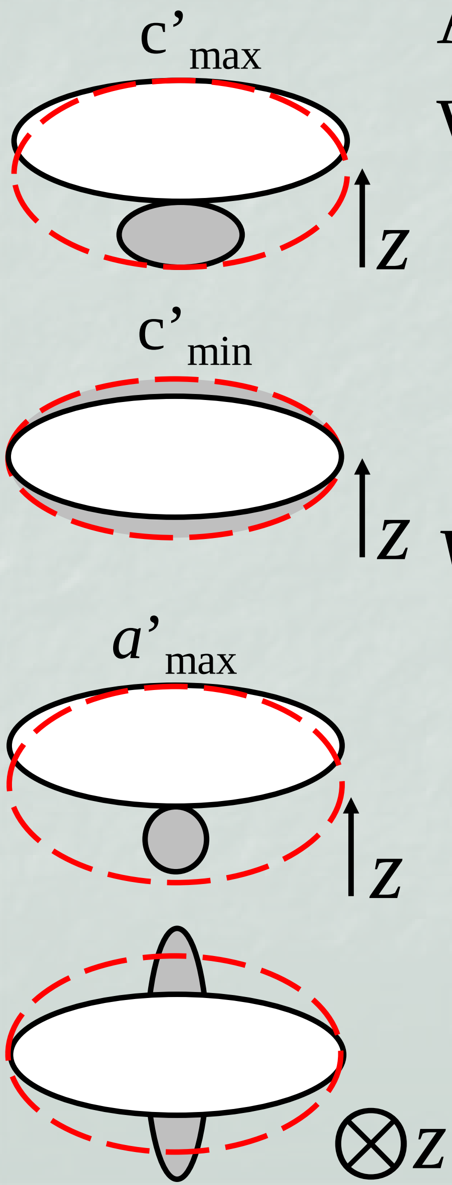

Assume $D_j \geqq D_k$

We determine $\rho^{\mathrm{i}}_j{}'$ by an interpolation

$$\rho_j^{\mathrm{i}\prime} = \frac{(\rho^{\mathrm{i}}_{\mathrm{true}} - \bar{\rho}^{\mathrm{i}}_{jk})\rho^{\mathrm{i,max}}_{jk} + (\bar{\rho}^{\mathrm{i}}_{jk} - \rho^{\mathrm{i}}_{\mathrm{crt}})\rho^{\mathrm{i,min}}_{jk}}{\rho^{\mathrm{i}}_{\mathrm{true}} - \rho^{\mathrm{i}}_{\mathrm{crt}}},$$

$$\rho^{\mathrm{i,max}}_{jk} = \bar{\rho}^{\mathrm{i}}_{jk}, \qquad \rho^{\mathrm{i,min}}_{jk} = \frac{m_j + m_k}{V_{\mathrm{max}}}.$$

V_{max} is given as follows

For $\phi_j \leq 1$ (collector is planar),

$$V_{\mathrm{max}} = (4\pi/3)a_j^2\{c_j + \min(a_k, c_k)\}.$$

For $\phi_j > 1$ (collector is columnar),

$$V_{\mathrm{max}} = (4\pi/3)c_j\{a_j + \min(a_k, c_k)\}\max(a_j, a_k, c_k).$$

4.2. Fluid Dynamics of Moist Air

Compressible Navier-Stokes eq. for moist air with coupling terms from particles

$$\frac{\partial \rho}{\partial t} + \nabla \cdot (\rho \boldsymbol{U}) = \underline{\left.\frac{\partial \rho}{\partial t}\right|_{\mathrm{cm}}},$$

mass coupling

$$\frac{\partial \rho q_{\mathrm{v}}}{\partial t} + \nabla \cdot (\rho q_{\mathrm{v}} \boldsymbol{U}) = \underline{\left.\frac{\partial \rho q_{\mathrm{v}}}{\partial t}\right|_{\mathrm{cm}}} + D_{\mathrm{v}} \nabla^2 (\rho q_{\mathrm{v}}),$$

$$\frac{\partial \rho \boldsymbol{U}}{\partial t} + \nabla \cdot (\rho \boldsymbol{U} \otimes \boldsymbol{U}) = -\nabla P - \rho g \hat{\boldsymbol{z}} + \underline{\left.\frac{\partial \rho \boldsymbol{U}}{\partial t}\right|_{\mathrm{cm}}} + \mu \nabla^2 \boldsymbol{U},$$

thermal coupling

momentum coupling

$$\frac{\partial \rho \theta}{\partial t} + \nabla \cdot (\rho \theta \boldsymbol{U}) = \underline{\left.\frac{\partial \rho \theta}{\partial t}\right|_{\mathrm{cm}}} + \frac{k}{c_{\mathrm{p}}} \nabla^2 \theta,$$

$$P = \rho R T = P_0 \left(\frac{\rho \theta R}{P_0}\right)^{c_{\mathrm{p}}/(c_{\mathrm{p}} - R)},$$

Coupling terms from particles

Mass coupling represents the source of vapor:

$$\left.\frac{\partial \rho}{\partial t}\right|_{\mathrm{cm}} = \left.\frac{\partial \rho q_{\mathrm{v}}}{\partial t}\right|_{\mathrm{cm}} = s_{\mathrm{v}} + s_{\mathrm{s}},$$

$$s_{\mathrm{v}}(\boldsymbol{x},t) = -\sum_{i\in I_{\mathrm{r}}(t)} \delta^3(\boldsymbol{x}-\boldsymbol{x}_i(t)) \left.\frac{dm_i}{dt}\right|_{\mathrm{cnd/evp}}, \quad s_{\mathrm{s}}(\boldsymbol{x},t) = -\sum_{i\in I_{\mathrm{r}}(t)} \delta^3(\boldsymbol{x}-\boldsymbol{x}_i(t)) \left.\frac{dm_i}{dt}\right|_{\mathrm{dep/sbl}}.$$

Thermal coupling represents heating due to the phase transition of water:

$$\left.\frac{\partial \rho\theta}{\partial t}\right|_{\mathrm{cm}} = -\frac{L_{\mathrm{v}} s_{\mathrm{v}} + L_{\mathrm{s}} s_{\mathrm{s}} + L_{\mathrm{f}} s_{\mathrm{f}}}{c_p \Pi},$$

$$\begin{aligned} s_{\mathrm{f}}(\boldsymbol{x},t) = &-\sum_{\text{freezing event } n} \delta^3(\boldsymbol{x}-\boldsymbol{x}_{i_n^{\mathrm{fz}}}(t))\delta(t-t_n^{\mathrm{fz}})m_{i_n^{\mathrm{fz}}}(t) \\ &+\sum_{\text{melting event } n} \delta^3(\boldsymbol{x}-\boldsymbol{x}_{i_n^{\mathrm{mlt}}}(t))\delta(t-t_n^{\mathrm{mlt}})m_{i_n^{\mathrm{mlt}}}(t) \\ &-\sum_{\text{riming event } n} \delta^3(\boldsymbol{x}-\boldsymbol{x}_{i_n^{\mathrm{rime}}}(t))\delta(t-t_n^{\mathrm{rime}})m_{i_n^{\mathrm{rime}}}(t). \end{aligned}$$

... Coupling terms from particles

Momentum coupling is the drag force from the particles:

$$\left.\frac{\partial \rho \boldsymbol{U}}{\partial t}\right|_{\mathrm{cm}} = -\sum_{i \in I_{\mathrm{r}}(t)} \delta^3(\boldsymbol{x} - \boldsymbol{x}_i(t))\boldsymbol{F}_i^{\mathrm{drg}}$$

$$\approx -\left[\sum_{i \in I_{\mathrm{r}}(t)} \delta^3(\boldsymbol{x} - \boldsymbol{x}_i(t)) m_i(t)\right] g\hat{\boldsymbol{z}}.$$

5. Numerical Schemes and Implementation of SCALE-SDM

We developed a numerical model SCALE-SDM to solve the time evolution equations of mixed-phase clouds.

5.1. Spatial Discretization of Moist Air

Prognostic variables: ρ, ρq_{v}, $\rho \boldsymbol{U}$, $\rho\theta$

Arakawa-C staggered grid (Arakawa and Lamb, 1977) is used

ρ, ρq_{v}, $\rho\theta$ are defined at the center of each grid cell, and $\rho \boldsymbol{U}$ are defined on the faces of each grid cell.

Hereafter, denoted by $\boldsymbol{G}_{lmn}$

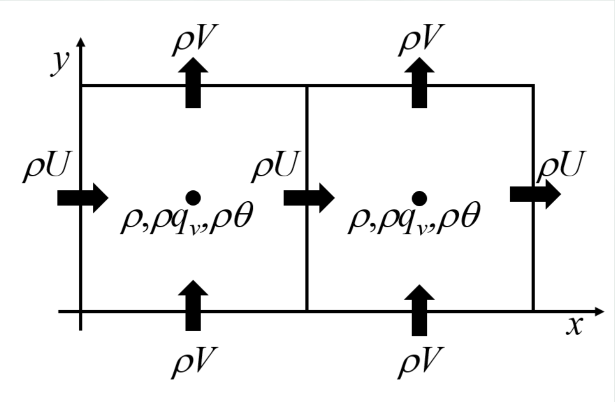

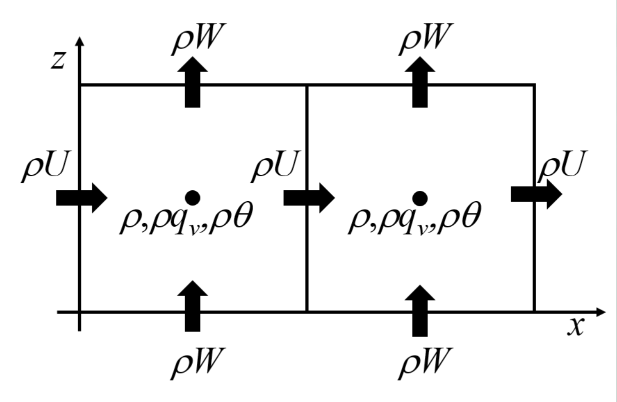

... Spatial discretization of moist air

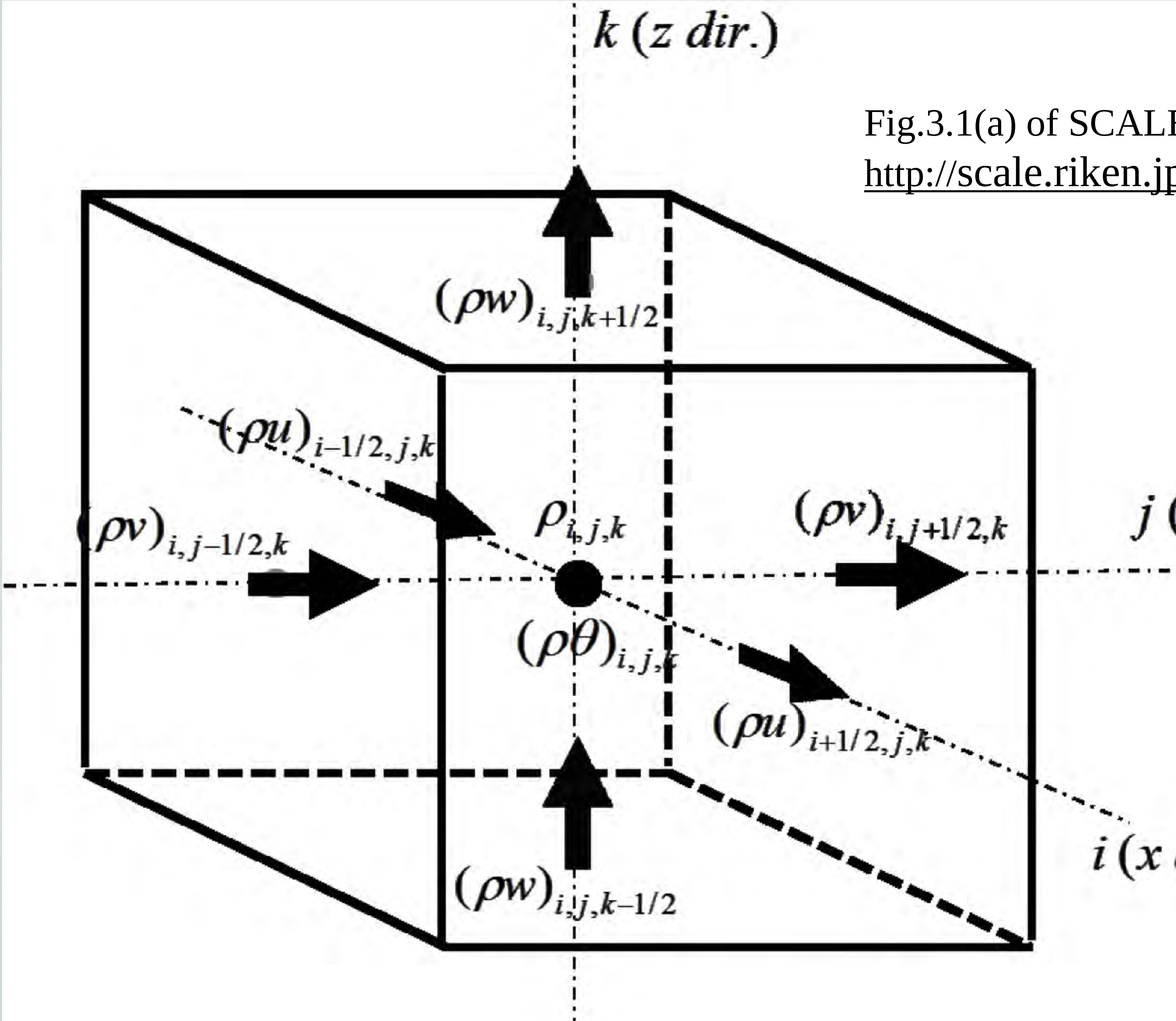

Fig.3.1(a) of SCALE-RM description, http://scale.riken.jp/doc/

5.2. Super-Particles and Real Particles

Fig.4 of Grabowski et al. (2019) (島作成)

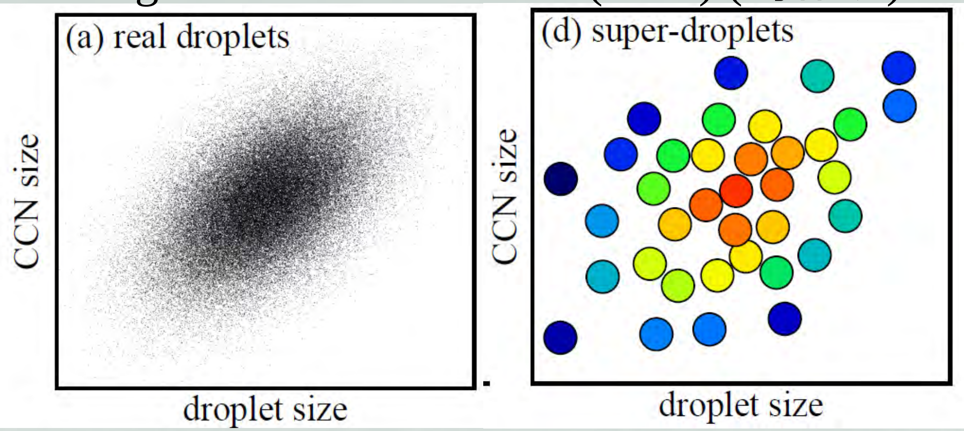

Real particles:

$$\{\{\boldsymbol{x}_i(t), \boldsymbol{a}_i(t)\}, \quad i = 1, 2, \ldots, N_{\mathrm{r}}^{\mathrm{wp}}\}$$

Super-particles (SPs)

Each SP has **multiplicity** ξ , position $\boldsymbol{x}$, and attribute $\boldsymbol{a}$

Each SP represents ξ number of real particles ($\boldsymbol{x}$,$\boldsymbol{a}$)

Population of real particles $\{(\boldsymbol{x}_i(t), \boldsymbol{a}_i(t)) | i=1,2,\ldots,N_r^{\mathrm{wp}}\}$ is represented by the SP population.

$$\{\{\xi_i(t), \boldsymbol{x}_i(t), \boldsymbol{a}_i(t)\}, i = 1, 2, \ldots, N_{\mathrm{s}}^{\mathrm{wp}}\}$$

N_s^{wp} is the num of SPs accumulated over all period

SP can be regarded as a weighted sample of real particles

Note that ξ is time dependent (Details later)

Relationship between SPs and real particles

Let $n(\boldsymbol{a}, \boldsymbol{x}, t)$ be the particle distribution function.

By definition, the following holds

$$n(\boldsymbol{a},\boldsymbol{x},t) = \left\langle \sum_{i\in I_\mathrm{r}(t)} \delta^d(\boldsymbol{a}-\boldsymbol{a}_i(t))\delta^3(\boldsymbol{x}-\boldsymbol{x}_i(t)) \right\rangle.$$

SPs reproduce the behavior of real particles in expectation:

$$\begin{aligned} n(\boldsymbol{a},\boldsymbol{x},t) &= \left\langle \sum_{i\in I_\mathrm{s}(t)} \xi_i(t)\delta^d(\boldsymbol{a}-\boldsymbol{a}_i(t))\delta^3(\boldsymbol{x}-\boldsymbol{x}_i(t)) \right\rangle \\ &= N_\mathrm{s}(t)\sum_{\xi=1}^{\infty}\xi p(\xi,\boldsymbol{a},\boldsymbol{x},t), \end{aligned}$$

where $p(\xi, \boldsymbol{a}, \boldsymbol{x}, t)$ is the probability density of SPs, $I_\mathrm{s}(t)$ is the set of SP indices existing in the domain at time t, and $N_\mathrm{s}(t)$ is the number of super-particles existing at time t.

5.3. Initialization of Super-Particles

Arbitrariness how to initialize SPs

Assume that initial $n(\boldsymbol{a}, \boldsymbol{x}, t=0)$ is given.

Any procedure that satisfies

$$n(\boldsymbol{a},\boldsymbol{x},0) = N_{\mathrm{s}}(0)\sum_{\xi=1}^{\infty}\xi p(\xi,\boldsymbol{a},\boldsymbol{x},0)$$

can be used to initialize SPs.

Uniform sampling method

Sample SPs uniform randomly from an interval. Then,

$$\xi(\boldsymbol{a},\boldsymbol{x}) = \frac{n(\boldsymbol{a},\boldsymbol{x},0)}{N_{\mathrm{s}}(0)p}, \quad p(\boldsymbol{a},\boldsymbol{x}) = p = \mathrm{const}.$$

(Constant multiplicity method) (not recommended)

If we set $\xi=N_{\mathrm{r}}(0)/N_{\mathrm{s}}(0)=\mathrm{const.}$, then $p(\boldsymbol{a}, \boldsymbol{x}, 0) \propto n(\boldsymbol{a}, \boldsymbol{x}, 0)$.

(Discrepancy) (e.g., Niederreiter, 1978)

Discrepancy of a set $P = \{x_1, \ldots, x_N\}$ is defined as

$$D_N(P) = \sup_{B \in J} \left| \frac{\#(B;P)}{N} - \lambda(B) \right|$$

In plain language, **"largest empty rectangular region that does not contain any points"**

from Carter (201

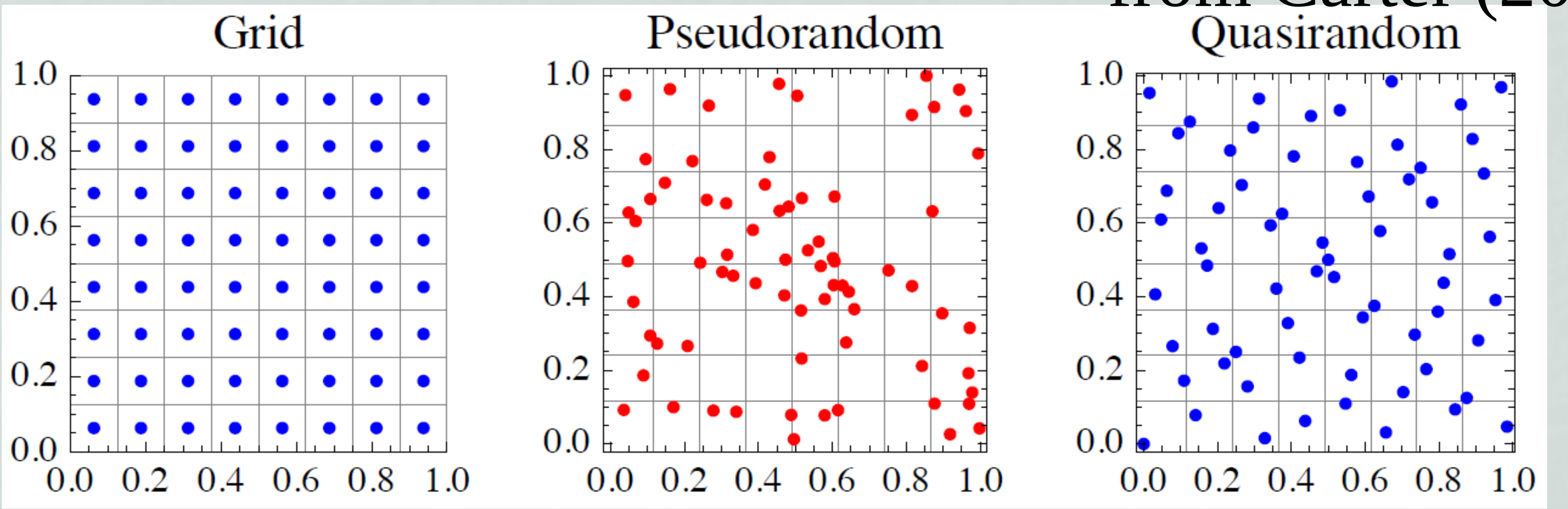

$D_N \propto N^{-1/s}$ $\quad D_N \propto N^{-1/2}$ $\quad D_N \propto (\log N)^s / N$

***s* is the dimension. Grid should not be used for $s \geqq 3$**

5.4. Operator Splitting of the Time Integration

Time integration of the system from t to $t+\Delta t$

We update each process separately

Let Δt be the common time step. The figure shows how $\{\{\xi_i, \boldsymbol{x}_i, \boldsymbol{a}_i\}\}$ and $\boldsymbol{G}_{lmn}$ are updated from time t to $t+\Delta t$

Let Δt_{adv}, $\Delta t_{\mathrm{fz/mlt}}$, $\Delta t_{\mathrm{cnd/evp}}$, $\Delta t_{\mathrm{dep/sbl}}$, and $\Delta t_{\mathrm{collis}}$ be the time steps for cloud microphysics processes.

Let Δt_{dyn} be the time step for fluid dynamics.

$t \longrightarrow t+\Delta t$

<table>
<tr><td>fluid dynamics</td><td>1</td><td>2</td><td>3</td><td>4</td><td>5</td><td>6</td></tr>
<tr><td>advection</td><td colspan="6">7</td></tr>
<tr><td>freezing/melting</td><td colspan="6">8</td></tr>
<tr><td>condensation/evaporation</td><td>9</td><td>12</td><td>13</td><td>15</td><td>17</td><td>19</td></tr>
<tr><td>deposition/sublimation</td><td colspan="2">10</td><td colspan="2">14</td><td colspan="2">18</td></tr>
<tr><td>collision-coalescence/riming/aggregation</td><td colspan="3">11</td><td colspan="3">16</td></tr>
</table>

... Time integration of the system from t to $t+\Delta t$

We first update $\boldsymbol{G}_{lmn}(t)$ to $\boldsymbol{G'}_{lmn}(t)$ but without coupling terms

Then we update $\{\{\xi_i,\boldsymbol{x}_i,\boldsymbol{a}_i\}\}$ from t to $t+\Delta t$

Processes lagging in time are calculated preferentially.

Simultaneously, we evaluate feedback from the particles to moist air, and update $\boldsymbol{G'}_{lmn}(t)$ to $\boldsymbol{G}_{lmn}(t+\Delta t)$

Remark

Based on Trotter's factorization formula. Global error is $O(\Delta t)$

Employing higher order formula, accuracy can be improved

5.5. Time Integration of Cloud Microphysics

Interpolation of fluid variables

$\boldsymbol{G}_i := \boldsymbol{G}(\boldsymbol{x}_i)$, the ambient air state around SP i, is often needed.

For scalar variables (ρ, ρq_{v}, $\rho\theta$), we use the center-grid value.

For wind velocities $\boldsymbol{U}$, we interpolate them from face grid. (detail later)

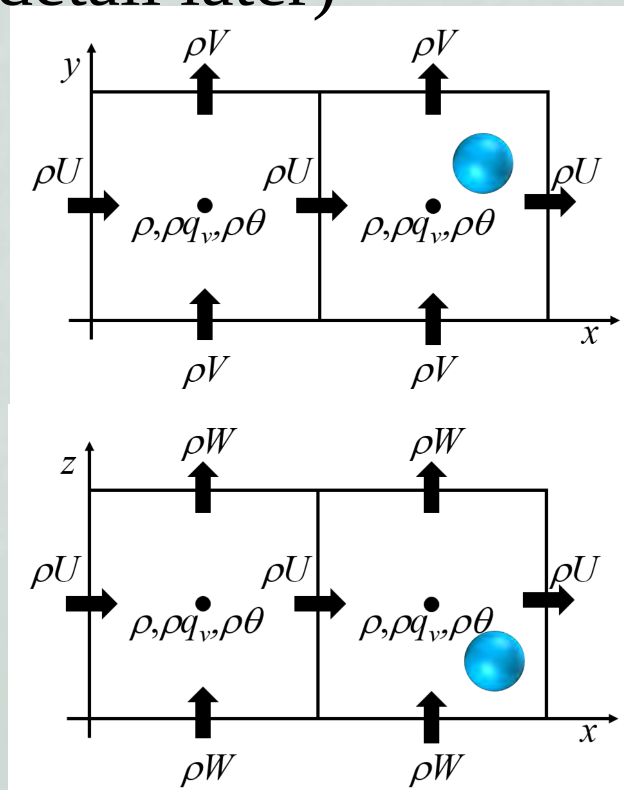

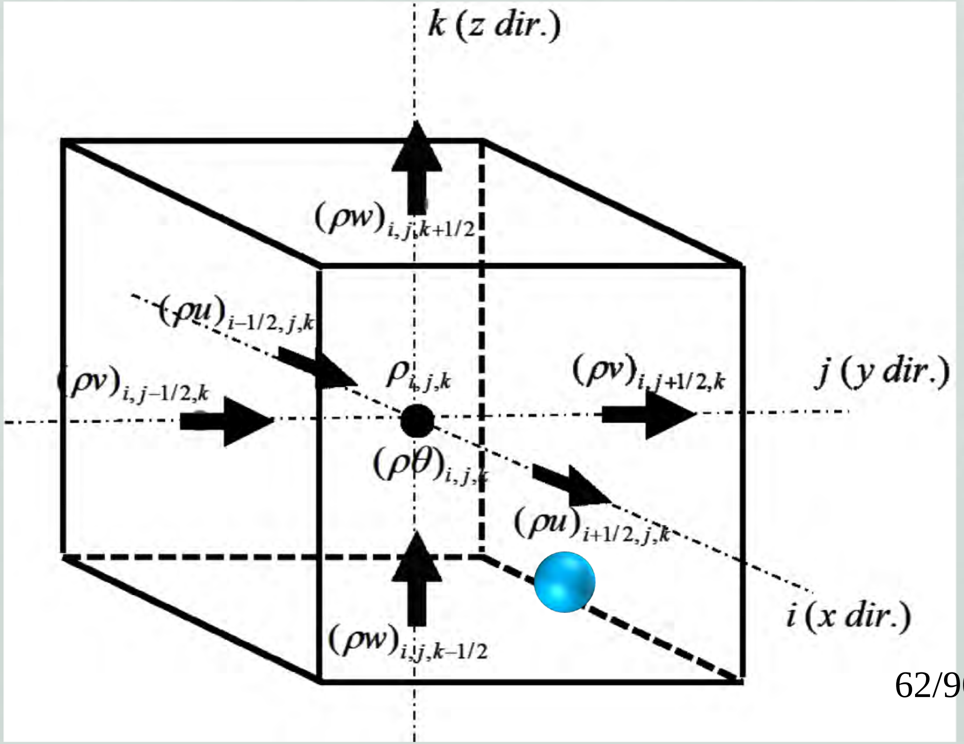

Motion of super-droplets

Basic equations

$$\boldsymbol{v}_i = \boldsymbol{U}_i - \hat{\boldsymbol{z}} v_i^\infty, \qquad \frac{d\boldsymbol{x}_i}{dt} = \boldsymbol{v}_i,$$

$$\left.\frac{\partial \rho \boldsymbol{U}}{\partial t}\right|_{\mathrm{cm}} \approx - \left[\sum_{i \in I_{\mathrm{r}}(t)} \delta^3(\boldsymbol{x} - \boldsymbol{x}_i(t)) m_i(t) \right] g \hat{\boldsymbol{z}}$$

Numerical scheme

Predictor-corrector scheme + “simple linear interpolation” of wind velocity (Grabowski et al., 2018)

In *x*-*z* 2D,

$$U_i = \alpha U_{l+1/2,n} + (1-\alpha) U_{l-1/2,n},$$
$$W_i = \gamma W_{l,n+1/2} + (1-\gamma) W_{l,n-1/2}.$$

This is for consistency of wind velocity divergence

In short, this enables more accurate calculation of droplet num density

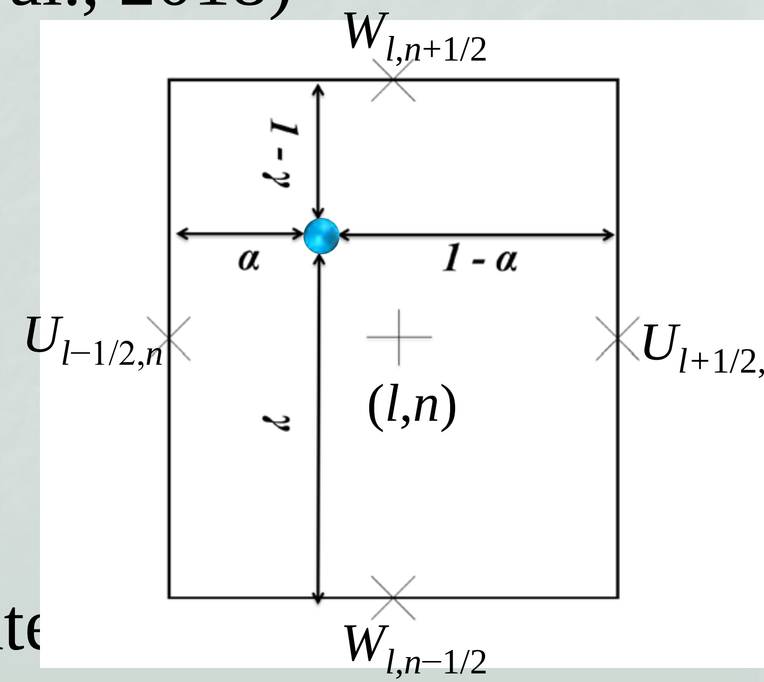

Fig.3 of Grabowski et al. (2018) with modification

... Motion of super-droplets

... Numerical scheme

The reaction force from each super-droplet is imposed on the nearest $(\rho W)_{lmn}$

Time step restriction

To accurately trace the flow of moist air, Δt_{adv} should be limited by the CFL condition of wind velocity.

Freezing and melting

Basic equations

Freezing occurs immediately when

(1) $e_i < e_s^{w}(T_i)$: supersaturated over liquid water; and

(2) $T_i < T_i^{fz}$: colder than the freezing temperature.

When $T_i > 0$°C, melting occurs immediately.

$$\left.\frac{\partial \rho\theta}{\partial t}\right|_{\mathrm{cm}} = -\frac{L_{\mathrm{f}} s_{\mathrm{f}}}{c_p \Pi}.$$

$$s_{\mathrm{f}}(\boldsymbol{x},t) = -\sum_{\text{freezing event } n} \delta^3(\boldsymbol{x} - \boldsymbol{x}_{i_n^{\mathrm{fz}}}(t))\delta(t - t_n^{\mathrm{fz}}) m_{i_n^{\mathrm{fz}}}(t) + \sum_{\text{melting event } n} \delta^3(\boldsymbol{x} - \boldsymbol{x}_{i_n^{\mathrm{mlt}}}(t))\delta(t - t_n^{\mathrm{mlt}}) m_{i_n^{\mathrm{mlt}}}(t).$$

Numerical scheme

We evaluate the above every $\Delta t_{\mathrm{fz/mlt}}$

Time step restriction

$\Delta t_{\mathrm{fz/mlt}}$ has to satisfy the CFL condition of wind velocity

Condensation and evaporation

Basic equations

$$r_i \frac{dr_i}{dt} = \frac{1}{\rho^{\mathrm{w}}(F_{\mathrm{k}}^{\mathrm{w}} + F_{\mathrm{d}}^{\mathrm{w}})} \left\{ S_i^{\mathrm{w}} - \frac{e_{\mathrm{s}i}^{\mathrm{w,eff}}(T_i)}{e_{\mathrm{s}}^{\mathrm{w}}(T_i)} \right\},$$

$$\left.\frac{\partial \rho}{\partial t}\right|_{\mathrm{cm}} = \left.\frac{\partial \rho q_{\mathrm{v}}}{\partial t}\right|_{\mathrm{cm}} = s_{\mathrm{v}}, \quad \left.\frac{\partial \rho\theta}{\partial t}\right|_{\mathrm{cm}} = -\frac{L_{\mathrm{v}} s_{\mathrm{v}}}{c_p \Pi}.$$

$$s_{\mathrm{v}} = -\sum_{i \in I_{\mathrm{r}}(t)} \delta^3(\boldsymbol{x} - \boldsymbol{x}_i(t)) \left.\frac{dm_i}{dt}\right|_{\mathrm{cnd/evp}},$$

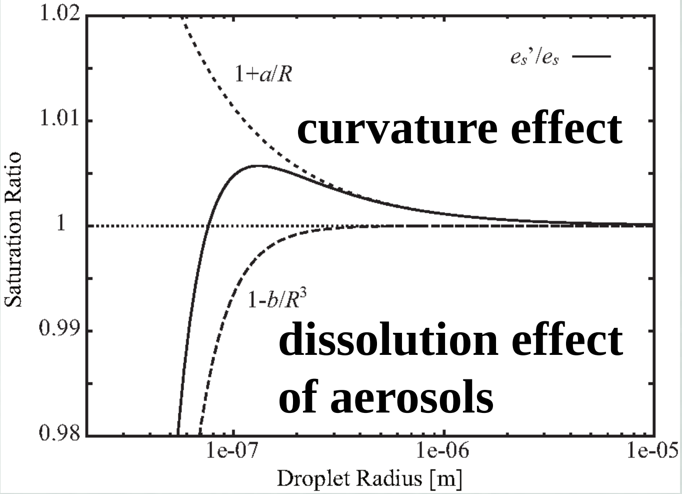

... Condensation and evaporation

- Numerical scheme
  - The activation/deactivation time scale is small.
  - To eliminate stiffness, we adopt the backward Euler scheme to the time evolution eq. of r^2 (SS et al., 2009).
  - Feedback from each super-droplet is imposed on the grid cell where the super-droplet is located.
- Time step restriction
  - The change of supersaturation through feedback is calculated explicitly.
  - Therefore, $\Delta t_{\mathrm{cnd/evp}}$ is restricted by the phase relaxation time (Squires, 1952), $\tau_{\mathrm{phase}} \propto 1/\sum \xi_i r_i$
  - Otherwise, numerical instability occurs (Árnason and Brown, 1971).

Deposition and sublimation

Basic equations

$$\frac{dm_i}{dt} = 4\pi C \frac{S_i^{\mathrm{i}} - 1}{F_{\mathrm{k}}^{\mathrm{i}} + F_{\mathrm{d}}^{\mathrm{i}}} \bar{f}_{\mathrm{vnt}}, \qquad \frac{dc_i}{da_i} = \Gamma(T_i) f_{\mathrm{vnt}} \frac{c_i}{a_i} =: \Gamma^* \frac{c_i}{a_i}, \qquad dV_i = \frac{dm_i}{\rho_{\mathrm{dep}}},$$

$$\left.\frac{\partial \rho}{\partial t}\right|_{\mathrm{cm}} = \left.\frac{\partial \rho q_{\mathrm{v}}}{\partial t}\right|_{\mathrm{cm}} = s_{\mathrm{s}}, \qquad \left.\frac{\partial \rho\theta}{\partial t}\right|_{\mathrm{cm}} = -\frac{L_{\mathrm{s}} s_{\mathrm{s}}}{c_p \Pi}, \qquad s_{\mathrm{s}}(\boldsymbol{x}, t) = -\sum_{i \in I_{\mathrm{r}}(t)} \delta^3(\boldsymbol{x} - \boldsymbol{x}_i(t)) \left.\frac{dm_i}{dt}\right|_{\mathrm{dep/sbl}}.$$

Numerical scheme

- Not stiffness because curvature term is ignored
- We adopt the forward Euler scheme.
- Feedback from each super-droplet is imposed on the grid cell where the super-droplet is located.

Time step restriction

- $\Delta t_{\mathrm{dep/sbl}}$ is also restricted by the phase relaxation time,

$$\tau_{\mathrm{phase}} \propto 1 / \sum \xi_i r_i$$

Coalescence, riming, aggregation

Stochastic collision-coalescence of real particles

$$P_{jk} = K(\boldsymbol{a}_j, \boldsymbol{a}_k; \boldsymbol{G})dt/\Delta V$$

Riming/aggregation outcome model

$$\left.\frac{\partial \rho\theta}{\partial t}\right|_{\mathrm{cm}} = -\frac{L_{\mathrm{f}} s_{\mathrm{f}}}{c_p \Pi}, \qquad s_{\mathrm{f}}(\boldsymbol{x}, t) = -\sum_{\text{riming event } n} \delta^3(\boldsymbol{x} - \boldsymbol{x}_{i_n^{\mathrm{rime}}}(t))\delta(t - t_n^{\mathrm{rime}}) m_{i_n^{\mathrm{rime}}}(t).$$

Numerical scheme

The Monte Carlo scheme of SDM (SS et al., 2009)

Time step restriction

$\Delta t_{\mathrm{collis}}$ is restricted by the mean free time of a (real) particle, i.e., the average time for a particle between two successive coalescence

$$\Delta t_{\mathrm{collis}} < 1/(n_{\mathrm{r}}\overline{K}),$$

where $\overline{K}$ is the typical value of the kernel.

5.6. Time Integration of the Moist Air Fluid Dynamics

Basic eq. (compressible Navier-Stokes eq. for moist air)

Fluid dynamics without the couplings is solved

$$\frac{\partial \rho}{\partial t} + \nabla \cdot (\rho \boldsymbol{U}) = \cancel{\left.\frac{\partial \rho}{\partial t}\right|_{\mathrm{cm}}},$$

$$\frac{\partial \rho q_{\mathrm{v}}}{\partial t} + \nabla \cdot (\rho q_{\mathrm{v}} \boldsymbol{U}) = \cancel{\left.\frac{\partial \rho q_{\mathrm{v}}}{\partial t}\right|_{\mathrm{cm}}} + D_{\mathrm{v}} \nabla^2 (\rho q_{\mathrm{v}}),$$

$$\frac{\partial \rho \boldsymbol{U}}{\partial t} + \nabla \cdot (\rho \boldsymbol{U} \otimes \boldsymbol{U}) = -\nabla P - \rho g \hat{\boldsymbol{z}} + \cancel{\left.\frac{\partial \rho \boldsymbol{U}}{\partial t}\right|_{\mathrm{cm}}} + \mu \nabla^2 \boldsymbol{U},$$

$$\frac{\partial \rho \theta}{\partial t} + \nabla \cdot (\rho \theta \boldsymbol{U}) = \cancel{\left.\frac{\partial \rho \theta}{\partial t}\right|_{\mathrm{cm}}} + \frac{k}{c_{\mathrm{p}}} \nabla^2 \theta,$$

$$P = \rho R T = P_0 \left(\frac{\rho \theta R}{P_0} \right)^{c_{\mathrm{p}}/(c_{\mathrm{p}} - R)},$$

Numerical schemes

For spatial discretization, the 4th-order central difference scheme is used for advection terms and the 2nd-order central difference scheme is used for other spatial derivatives. To preserve the monotonicity, the flux-corrected transport scheme of Zalesak (1979) is used for water vapor advection.

For time integration, the 3-step Runge–Kutta scheme of Wicker and Skamarock (2002) is used. An artificial, 4th-order hyper-diffusion term is added for stability.

For more detail, see the SCALE description document

https://scale.riken.jp/doc/index.html

Time step restriction

Δt_{dyn} must satisfy the CFL condition of acoustic waves.

6. Design of Cumulonimbus Simulation (2D)

CTRL ensemble

Sounding	Khain et al., Part I, JAS (2004)
Aerosol	pure $(NH_4)HSO_4$: 315/cc (3 × vanZanten et al., 2011) mineral dust+$(NH_4)HSO_4$: d^{dust}=1μm, 1/cc
Grid size	$\Delta x=\Delta y=\Delta z=62.5$m
SP number	128SPs/cell
Time steps	(Δt, Δt_{adv}, $\Delta t_{fz/mlt}$, Δt_{collis}, $\Delta t_{cnd/evp}$, $\Delta t_{dep/sbl}$, Δt_{dyn}) =(0.4s, 0.4s, 0.4s, 0.2s, 0.1s, 0.1s, 0.05s)
SGS Turbulence	None
Trials	10

Other ensembles

NSP: SP number convergence

DX: grid convergence

DT: time step convergence

7. Typical Behavior of CTRL ensemble

Results of the typical realization of CTRL is shown

Hydrometeor categorization for analysis

Partially melted ice is not considered in the present model

- cloud droplet: $r < 40\mu\mathrm{m}$
- rain droplet: $r \geqq 40\mu\mathrm{m}$
- graupel: $m^{\mathrm{rime}}/m > 0.3$
- snow aggregate: $m^{\mathrm{rime}}/m \leqq 0.3$ and $n^{\mathrm{mono}} > 10$
- cloud ice: other ice particles

Time evolution of water path and precipitation

Figs. 2 and 3 of SS et al. (2020)

Domain averaged water path

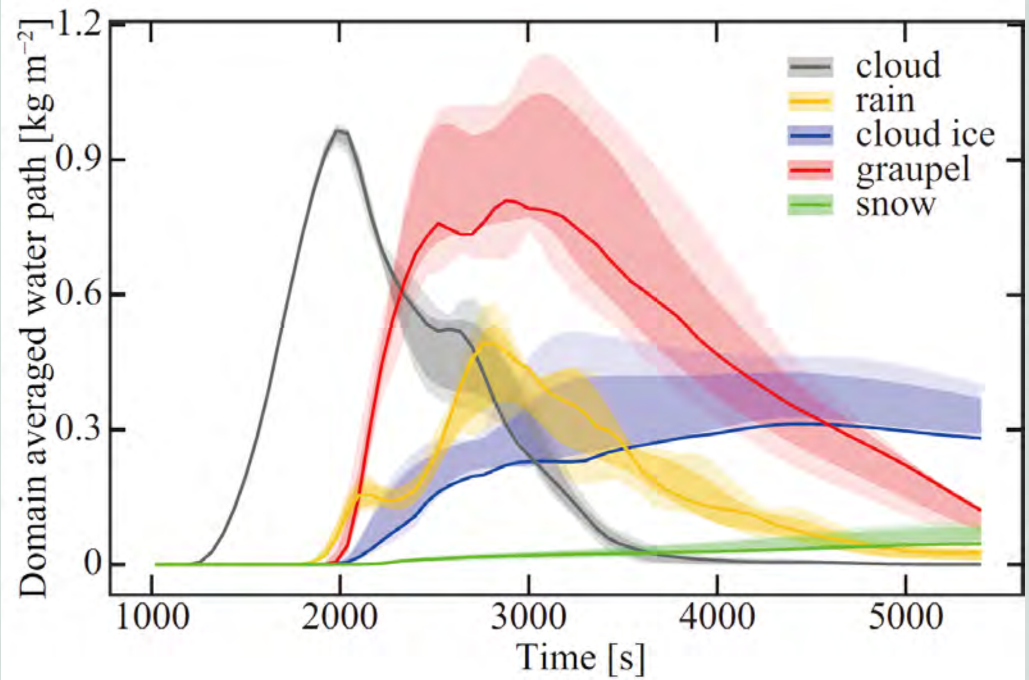

Domain averaged precipitation

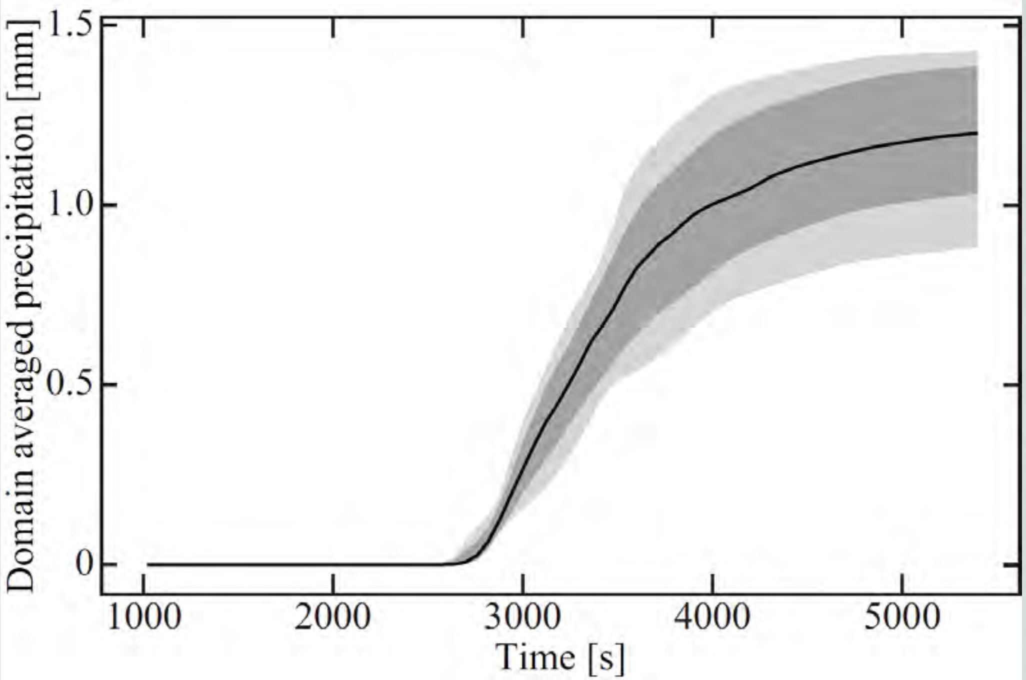

Solid line: typical representation of CTRL (defined as the member that produced precipitation closest to the mean)

Dark shade: mean ± standard deviation

Pale shade: max and min of the 10 members

Spatial structure of the cloud

white: cloud, yellow: rain, blue: cloud ice, red: graupel/hail, green: snow aggregate

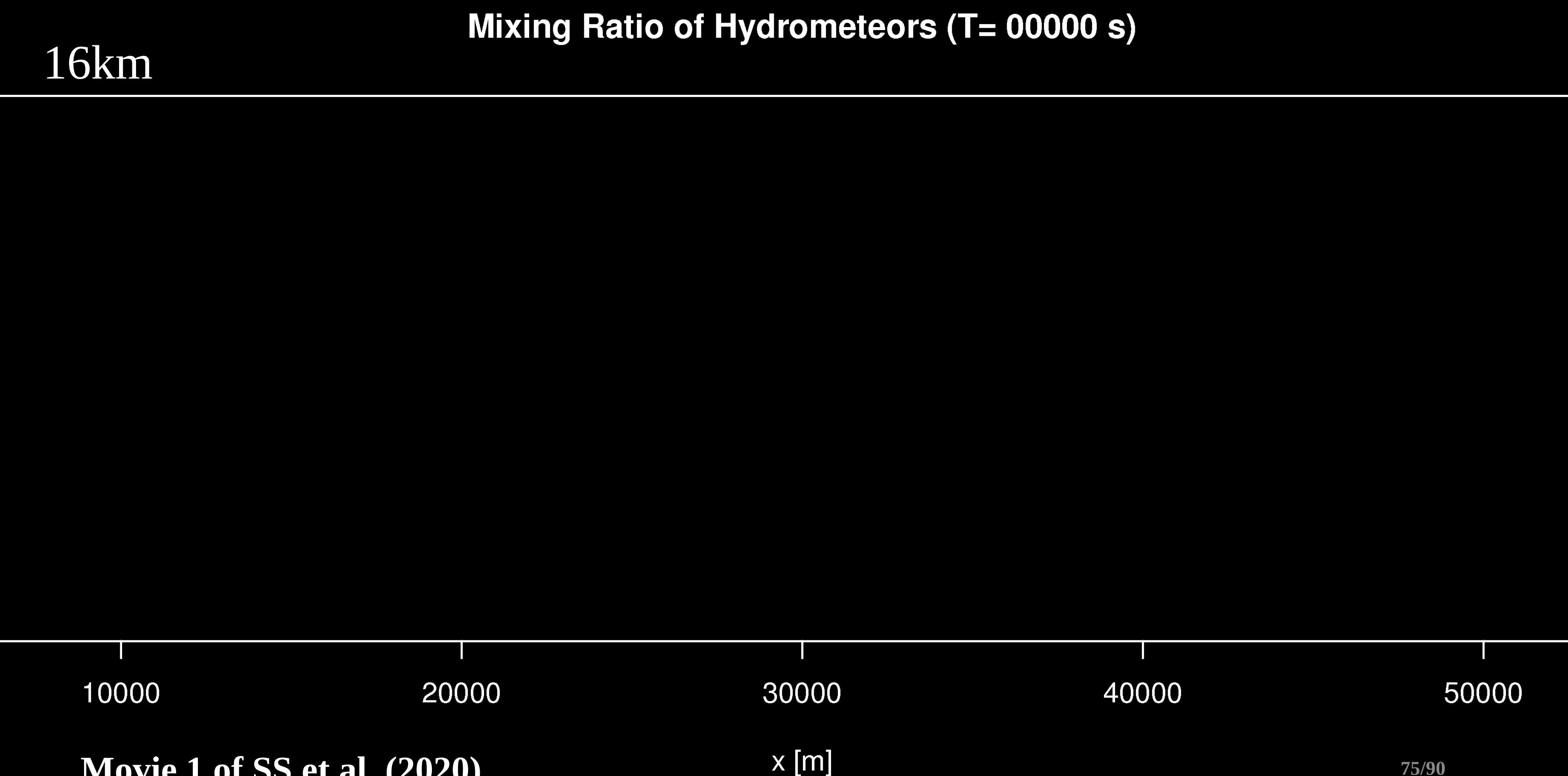

Movie 1 of SS et al. (2020)

... Spatial structure of the cloud

white: cloud, yellow: rain, blue: cloud ice, red: graupel/hail, green: snow aggregate

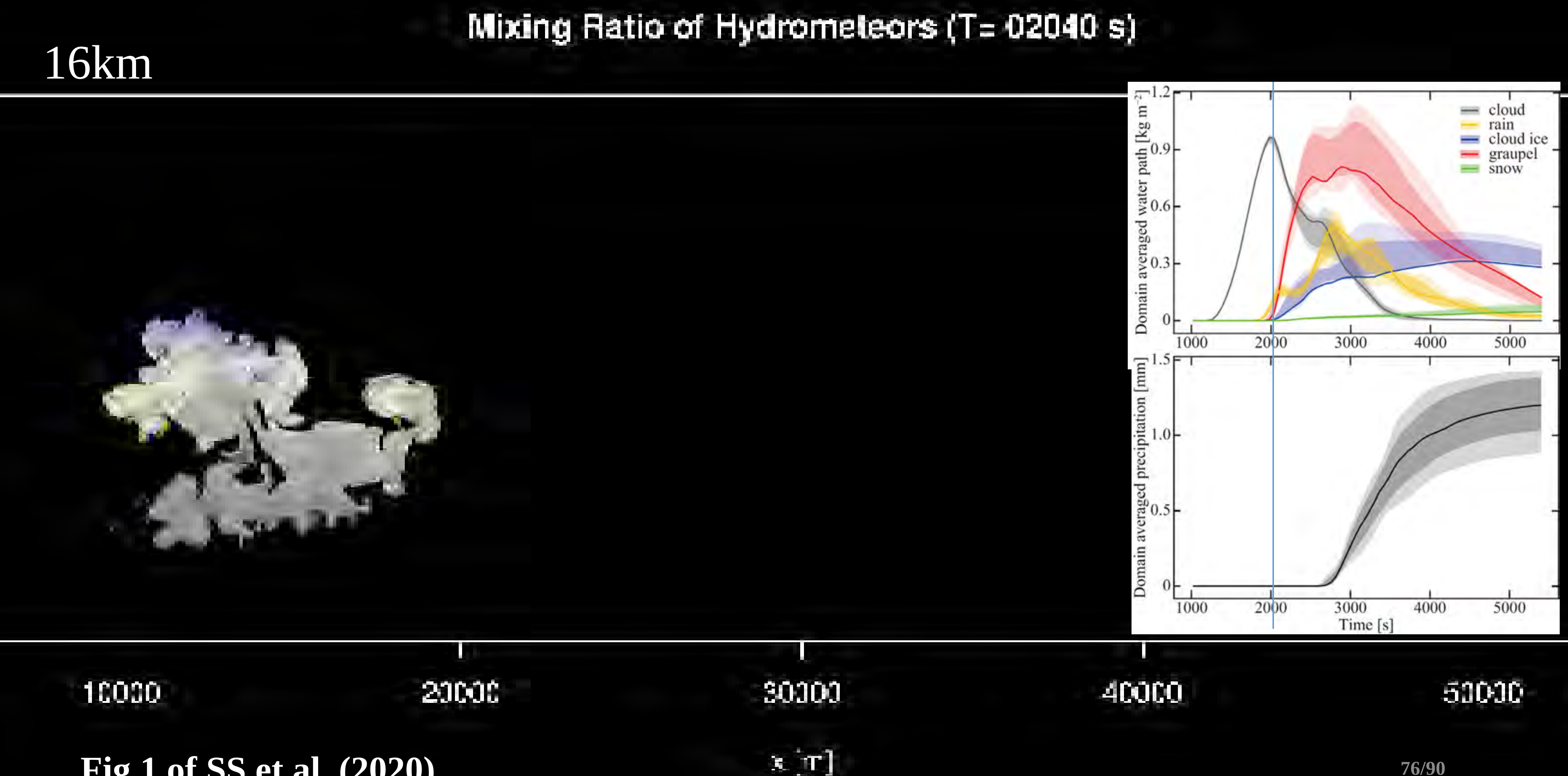

Fig.1 of SS et al. (2020)

... Spatial structure of the cloud

white: cloud, yellow: rain, blue: cloud ice, red: graupel/hail, green: snow aggregate

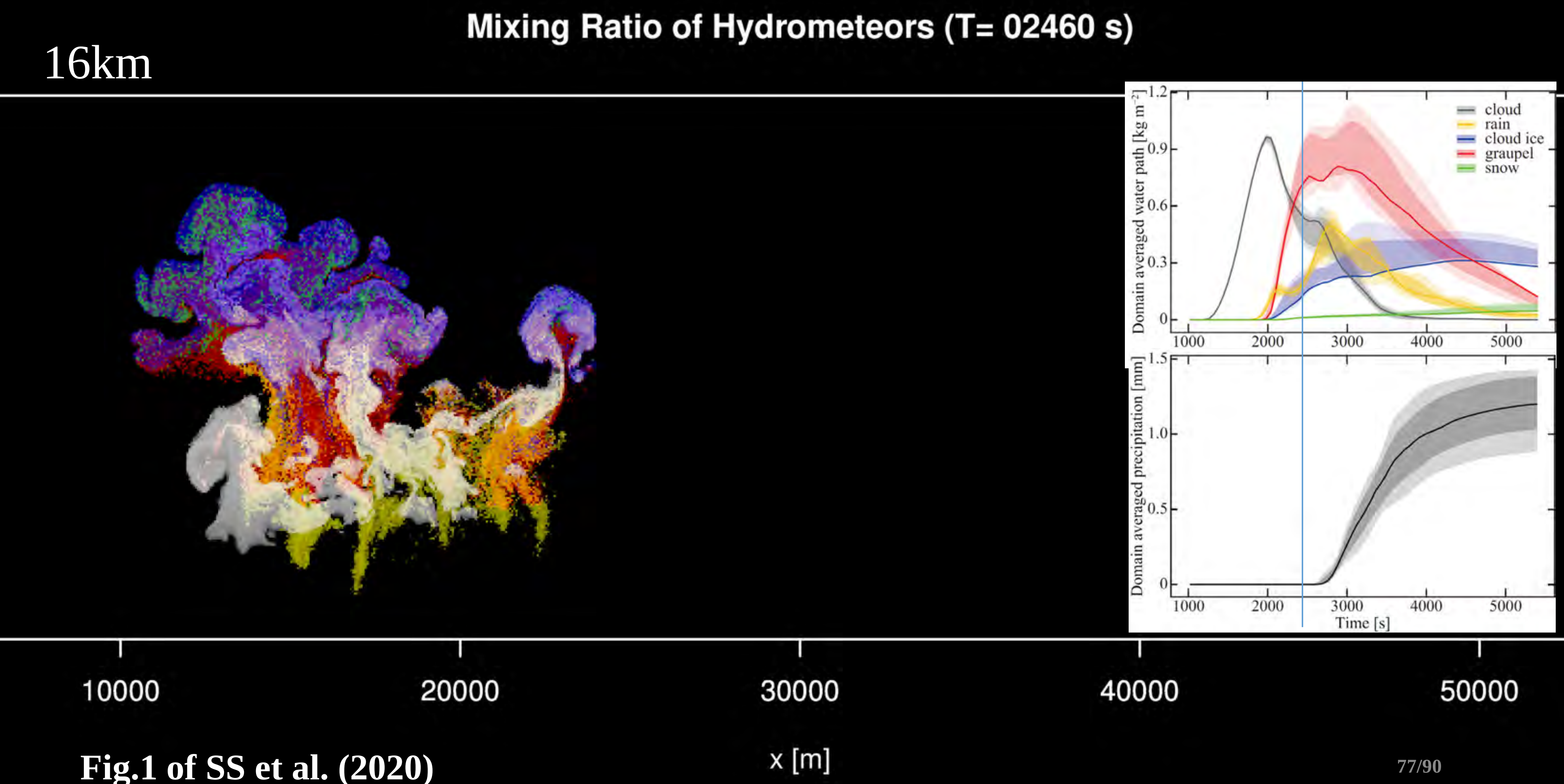

Fig.1 of SS et al. (2020)

... Spatial structure of the cloud

white: cloud, yellow: rain, blue: cloud ice, red: graupel/hail, green: snow aggregate

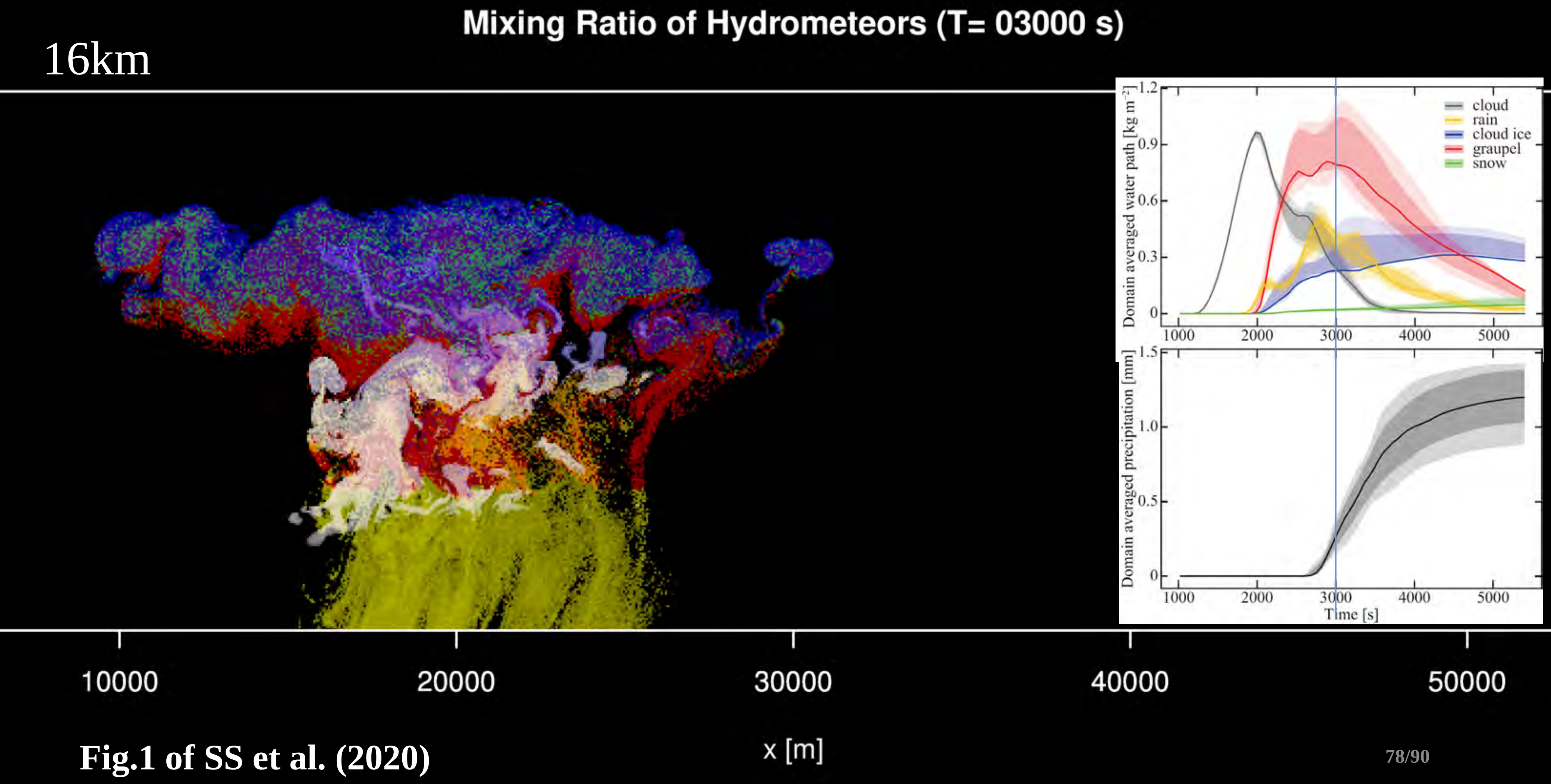

Fig.1 of SS et al. (2020)

... Spatial structure of the cloud

white: cloud, yellow: rain, blue: cloud ice, red: graupel/hail, green: snow aggregate

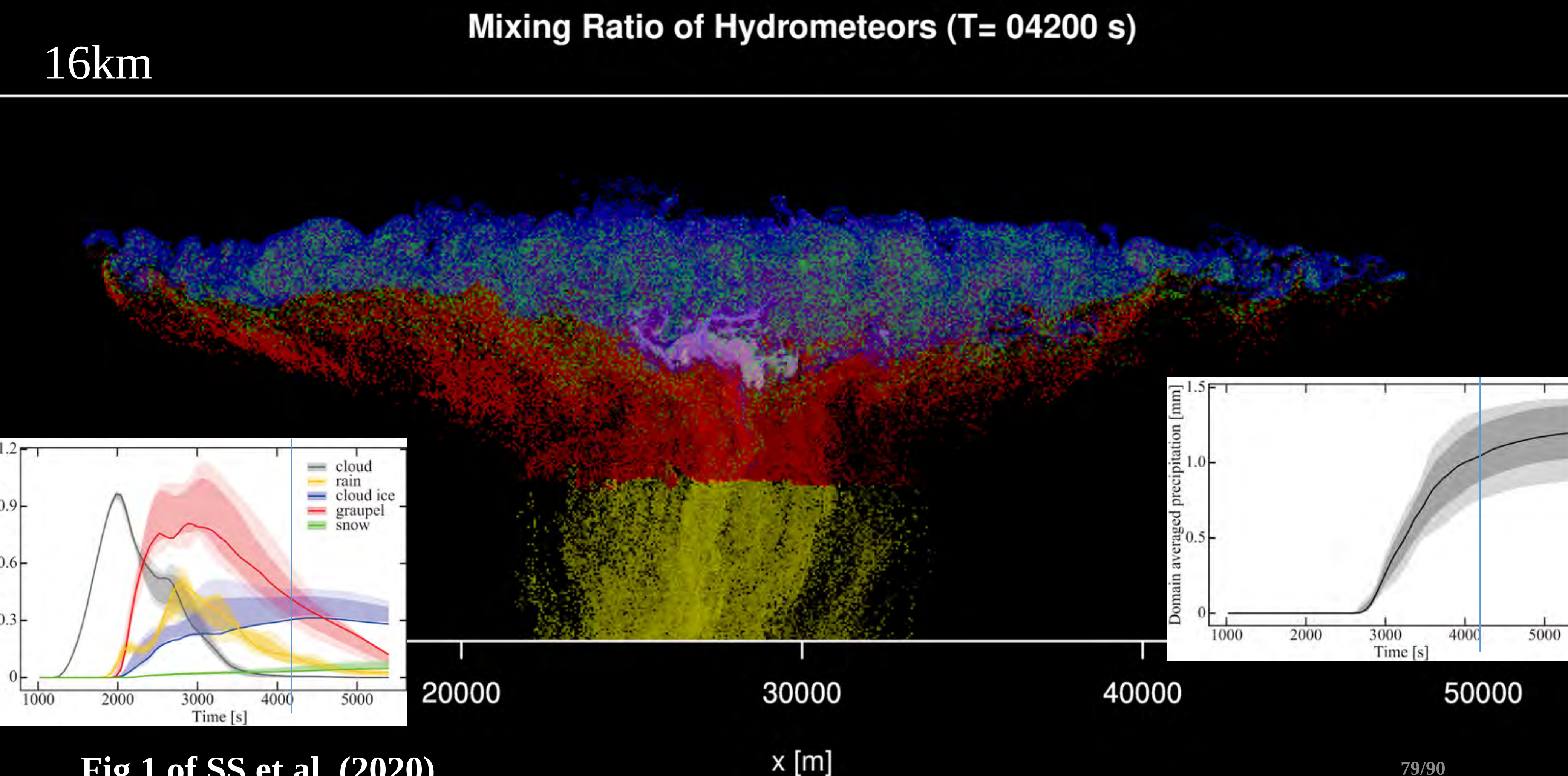

Fig.1 of SS et al. (2020)

... Spatial structure of the cloud

white: cloud, yellow: rain, blue: cloud ice, red: graupel/hail, green: snow aggregate

Typical life cycle was well reproduced

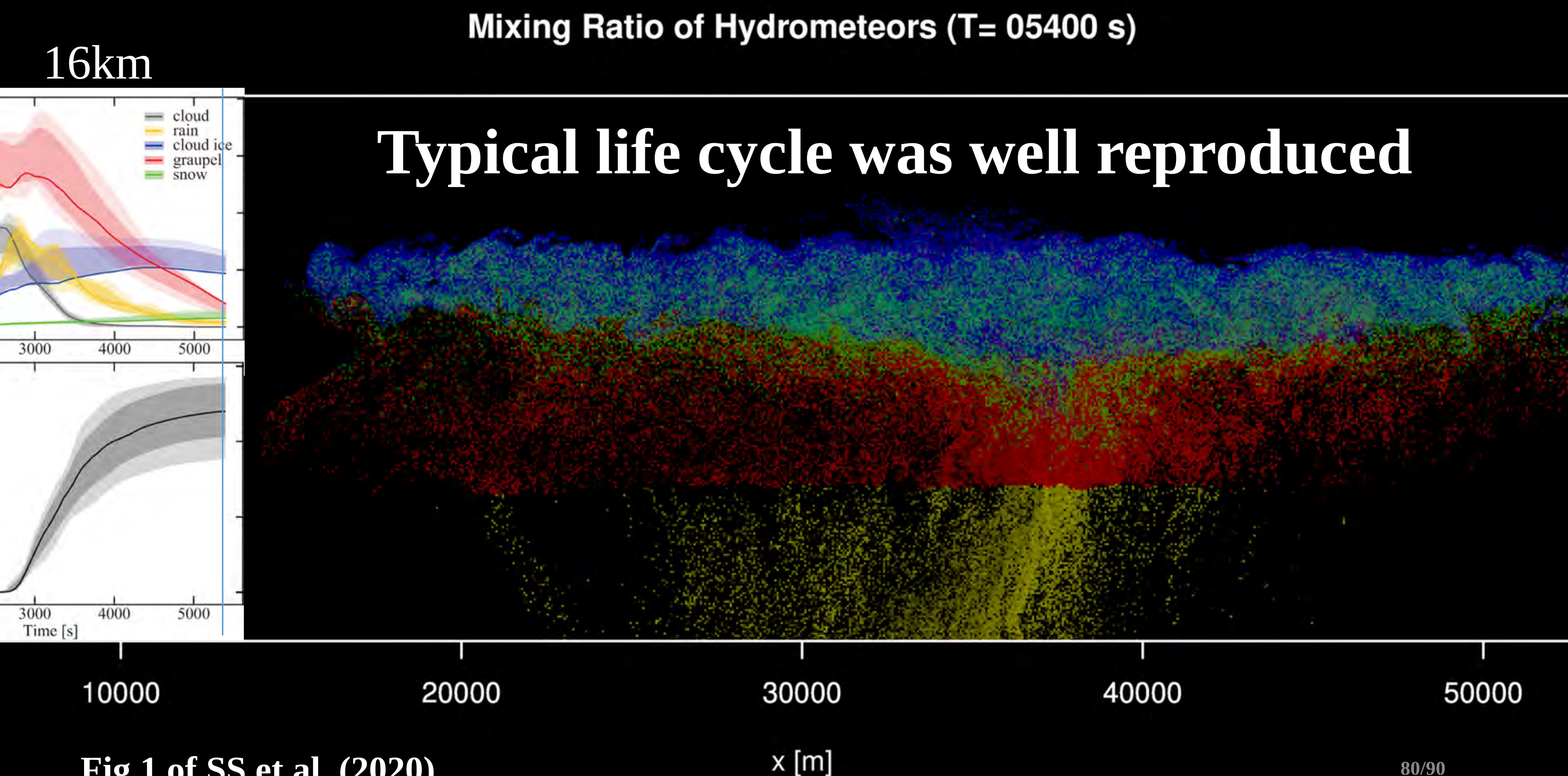

Fig.1 of SS et al. (2020)

Mass(M)- and Velocity(V)-Dimension(D) relationships

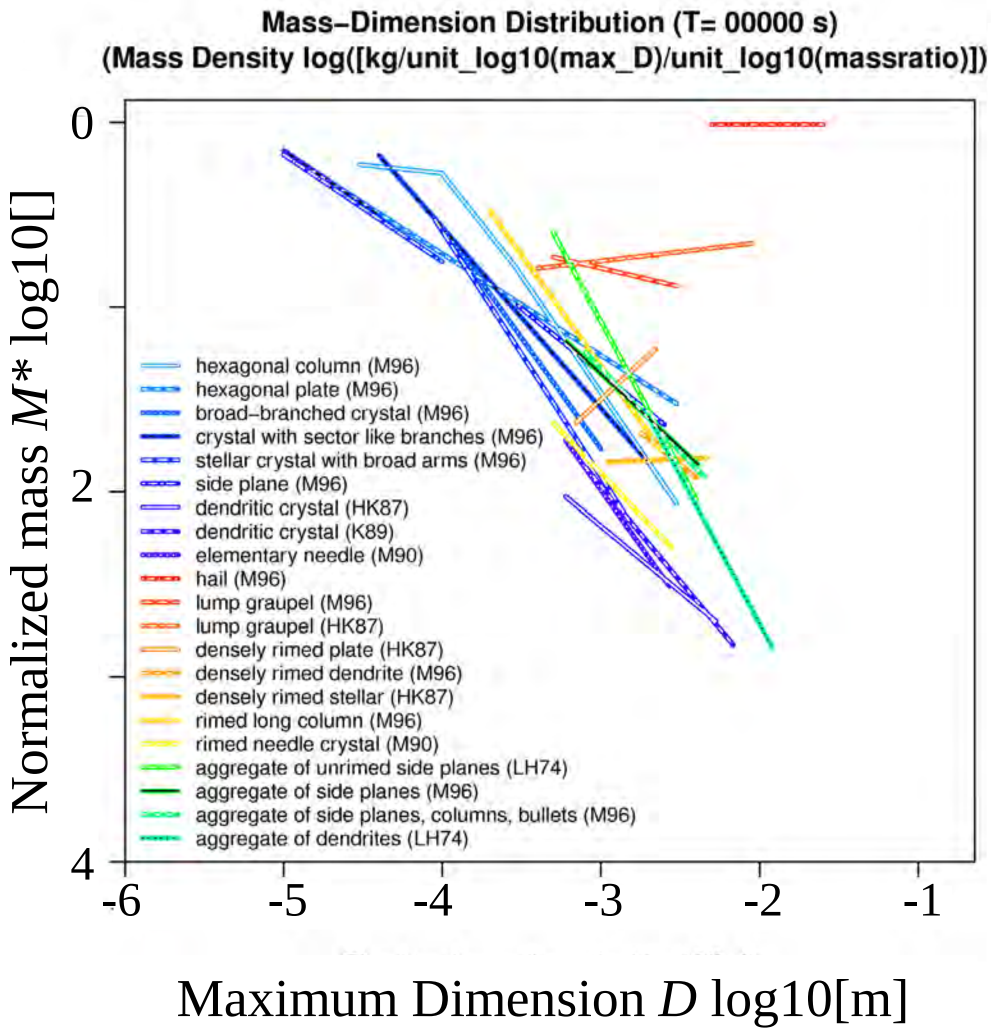

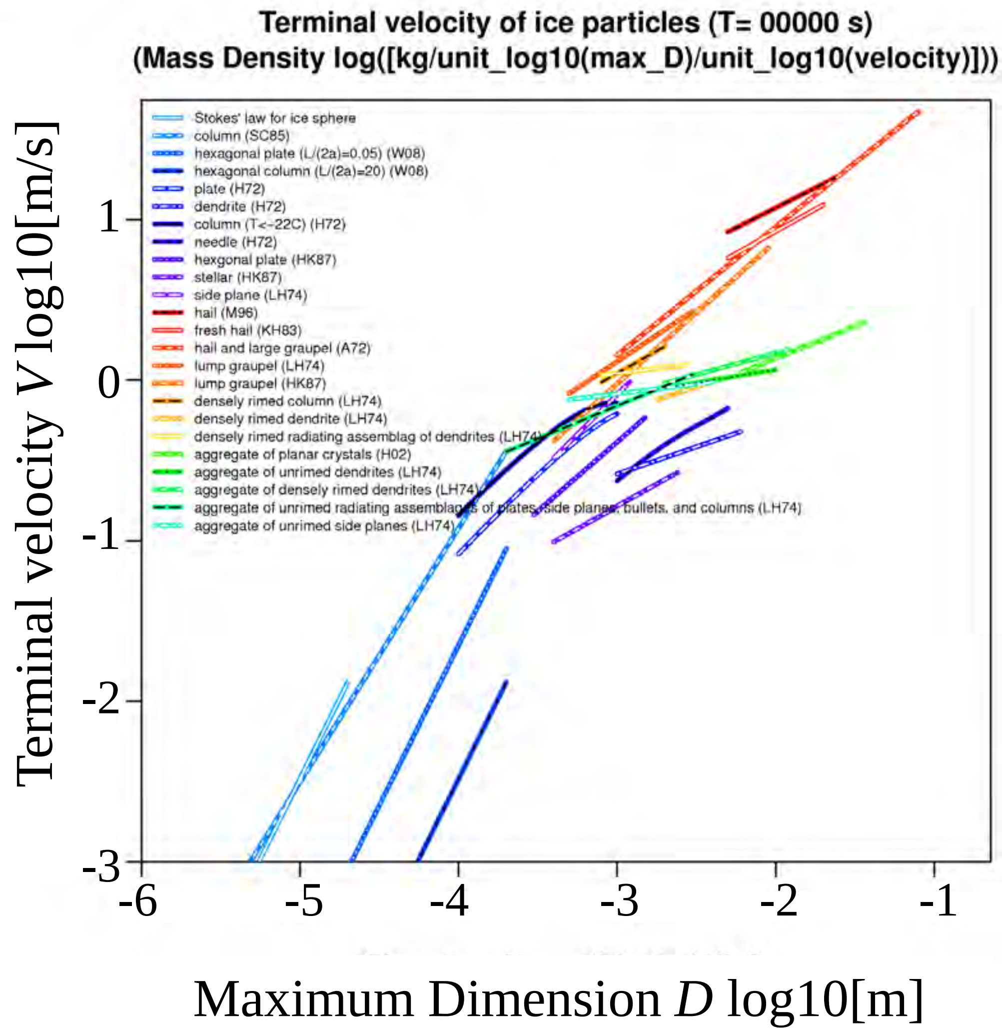

blue: cloud ice, red: graupel/hail, green: snow aggregate

Movies. 13 and 16 of SS et al. (2020)

Agrees fairly well existing formulas

... Mass(M)- and Velocity(V)-Dimension(D) relationships

T = 2040s (towering)

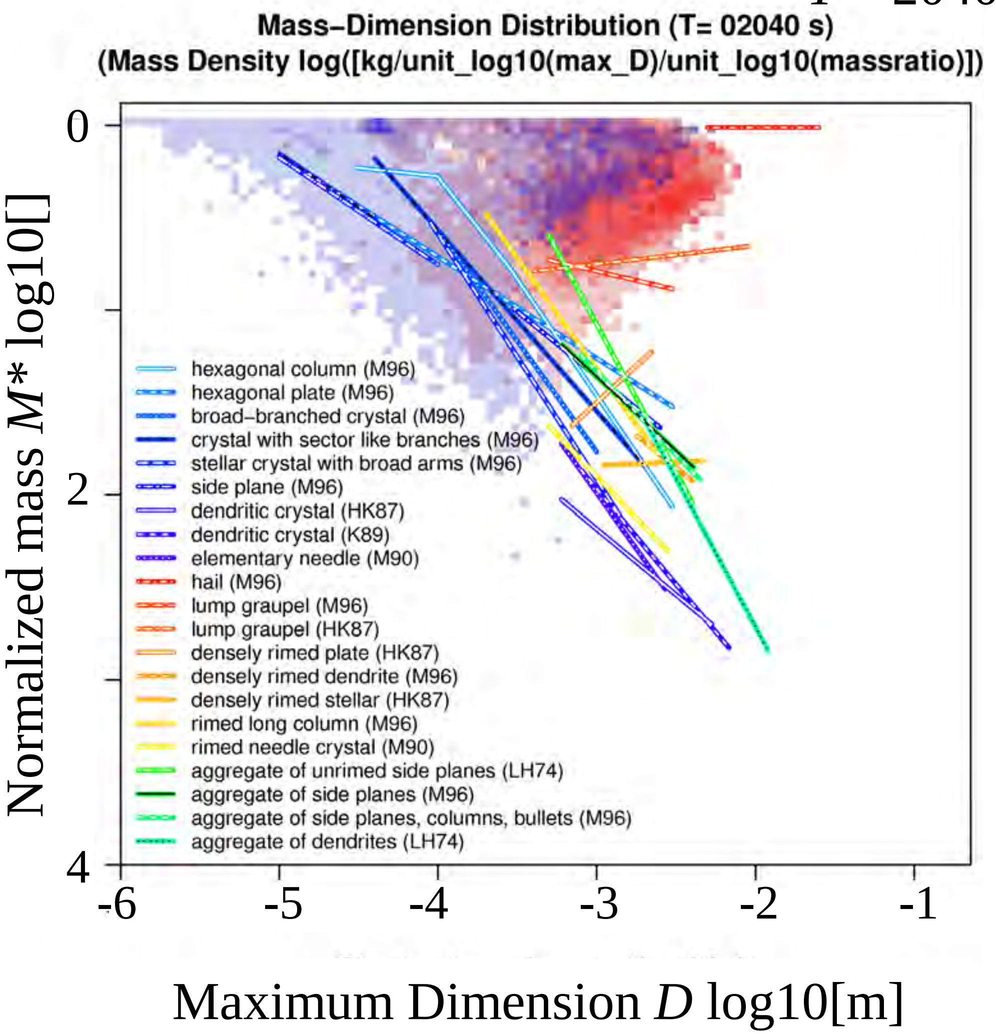

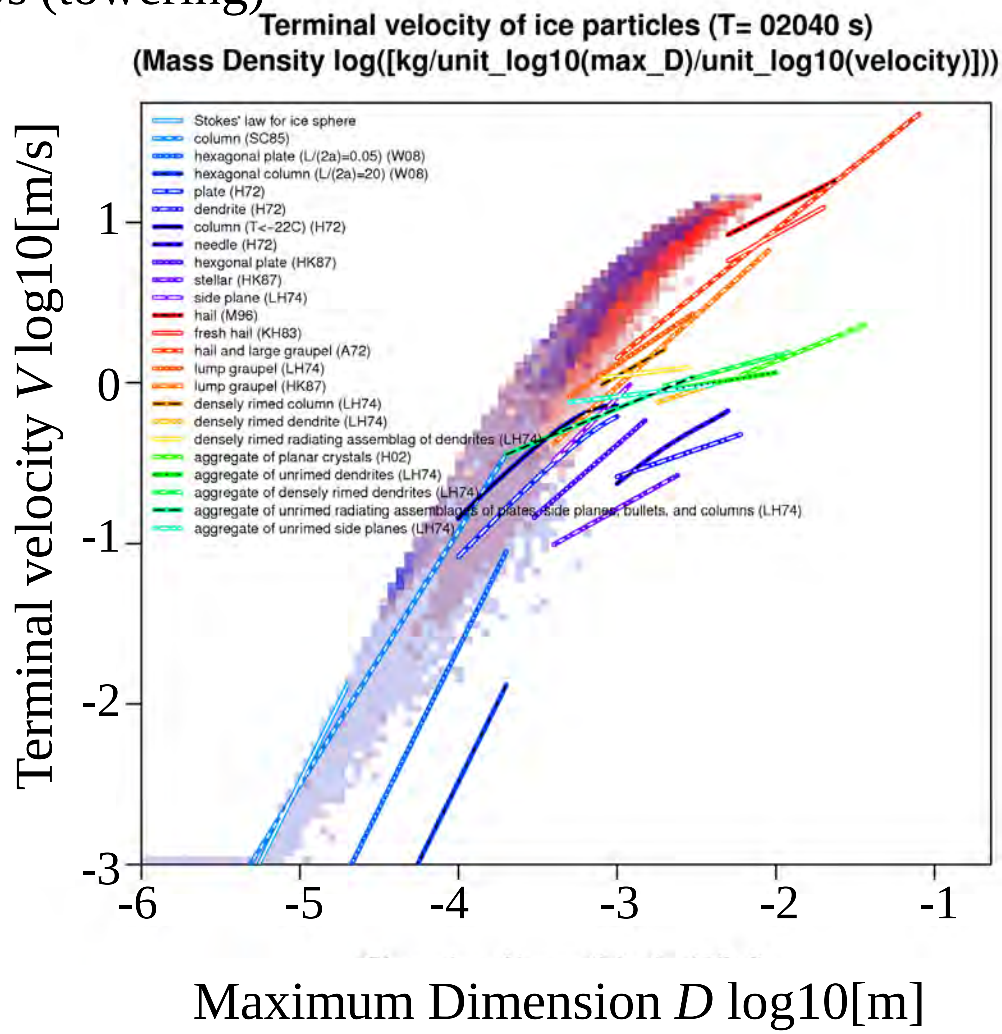

blue: cloud ice, red: graupel/hail, green: snow aggregate

Figs. R2-5 and R2-8 of SS et al. (2020)

Agrees fairly well existing formulas

... Mass(M)- and Velocity(V)-Dimension(D) relationships

T = 3000s (mature)

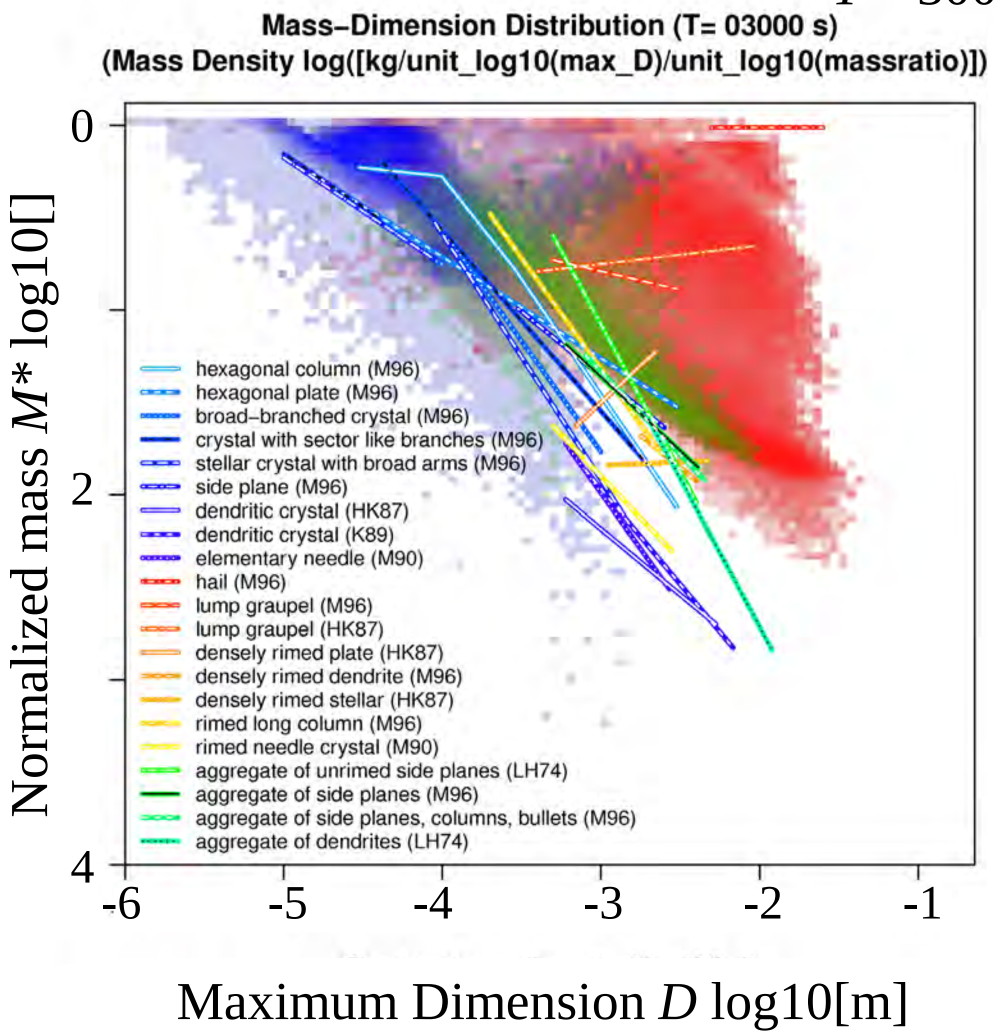

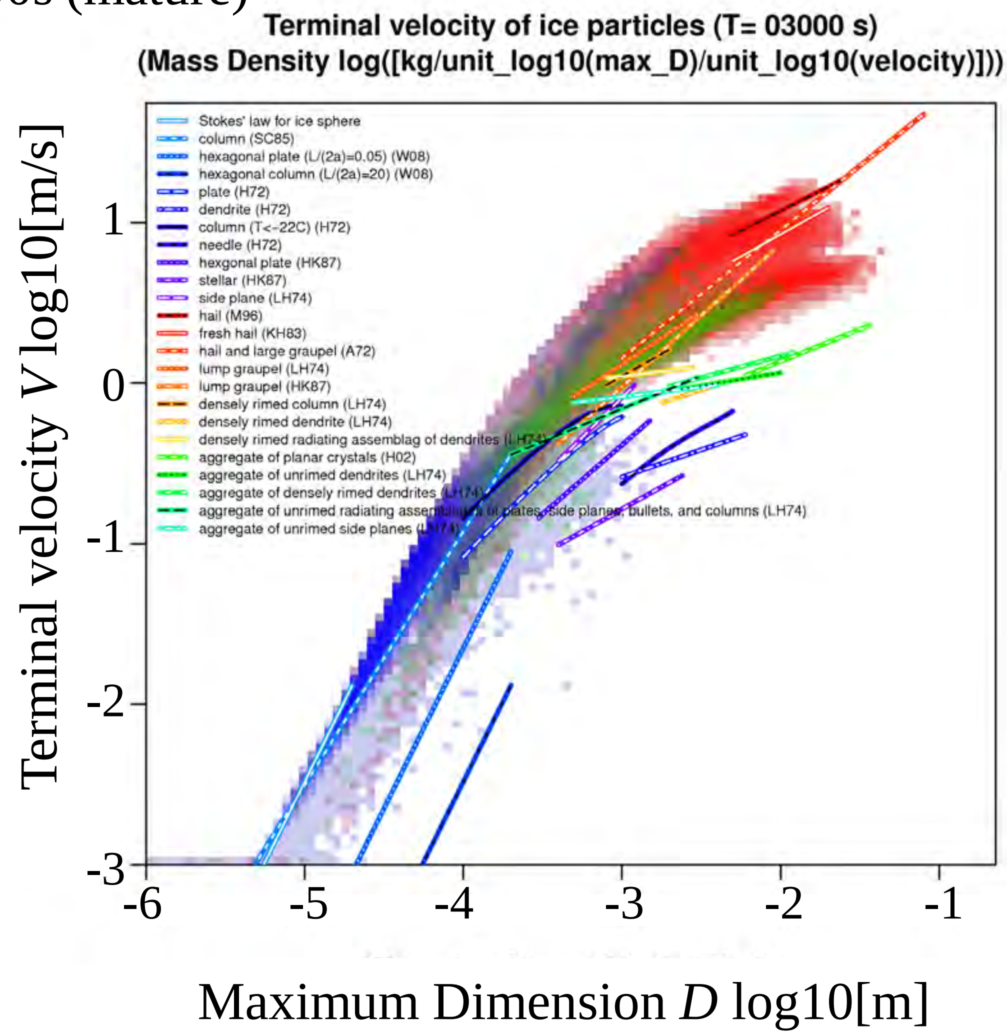

blue: cloud ice, red: graupel/hail, green: snow aggregate

Figs. R2-5 and R2-8 of SS et al. (2020)

Agrees fairly well existing formulas

... Mass(M)- and Velocity(V)-Dimension(D) relationships

T = 5400s (dissipating)

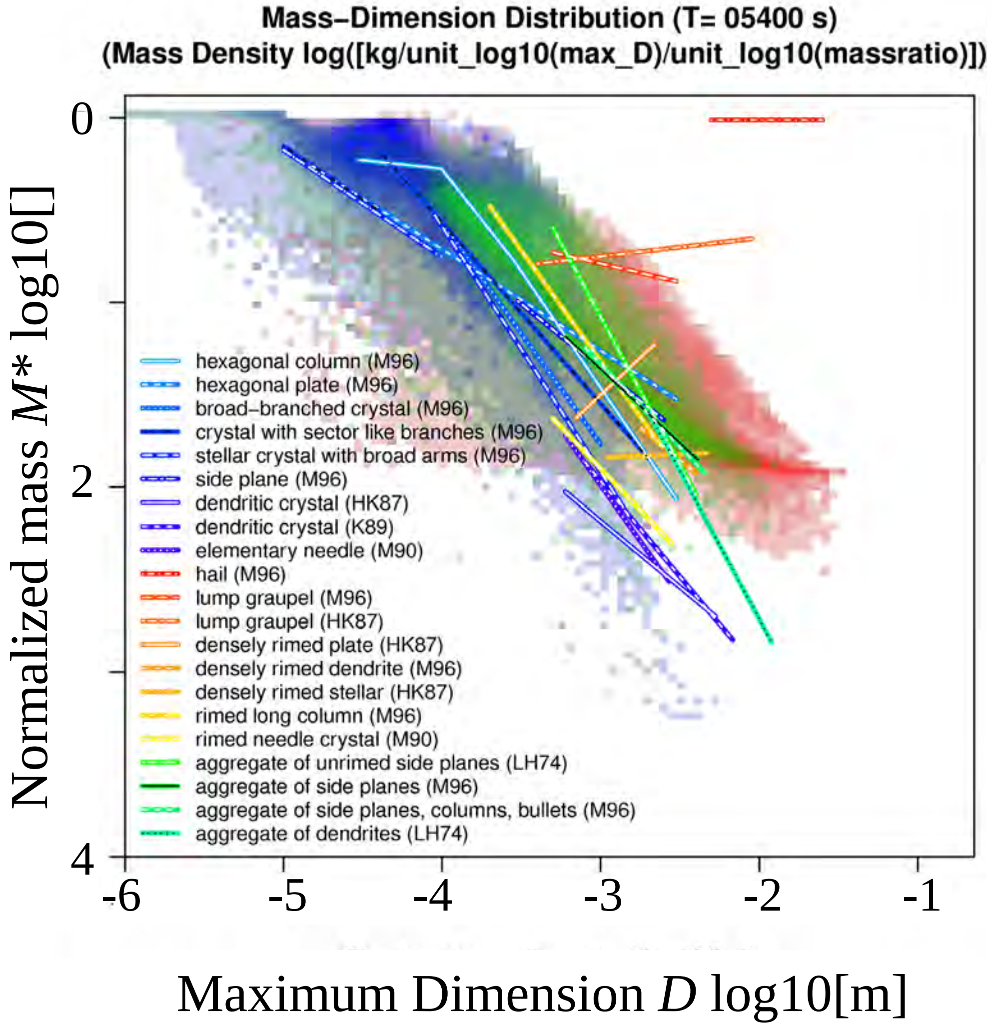

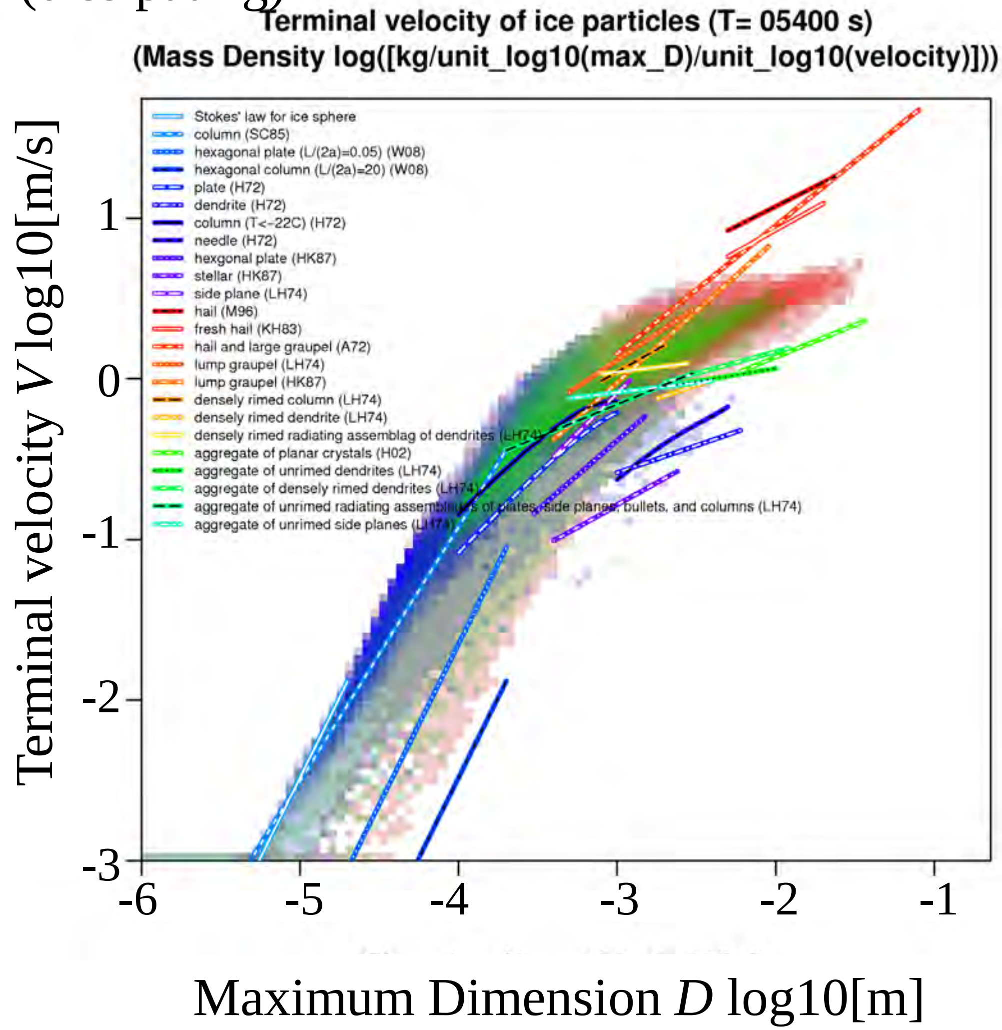

blue: cloud ice, red: graupel/hail, green: snow aggregate

Figs. R2-5 and R2-8 of SS et al. (2020)

Agrees fairly well existing formulas

8. Numerical Convergence Characteristics

SP number convergence

Precipitation amount

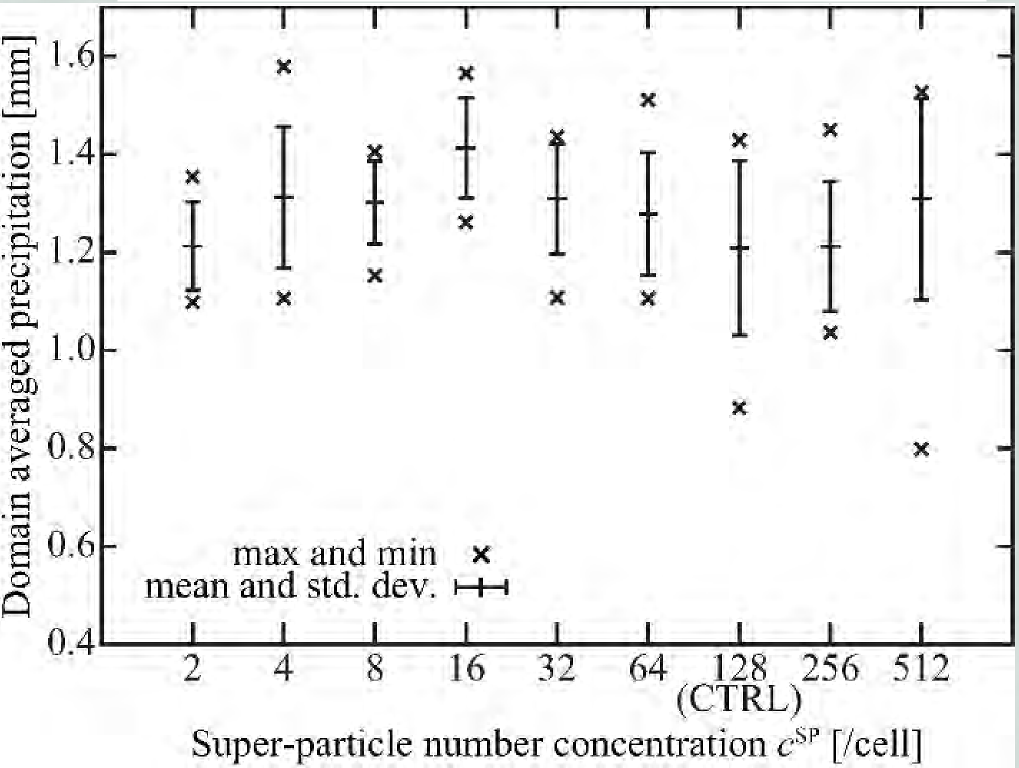

Max amount of each hydrometeor during the period

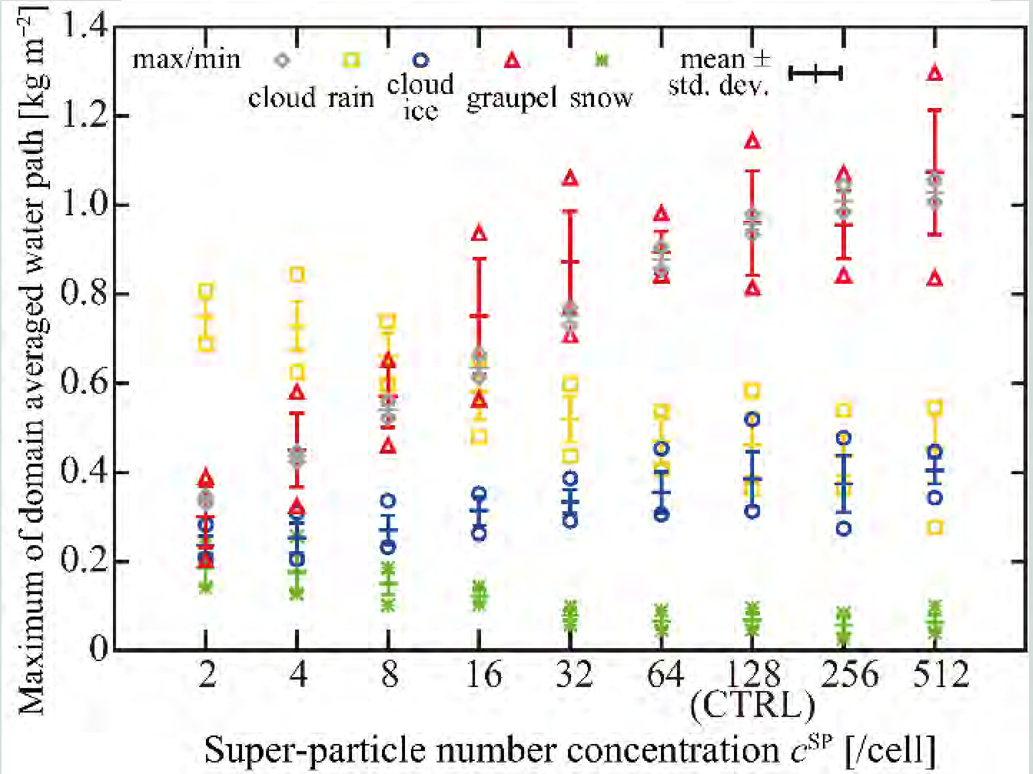

Figs. 8 and 9 of SS et al. (2020)

128 SPs/cell seems to be sufficient. (x30 computational cost than a two-moment bulk model.)

Grid convergence

Precipitation amount

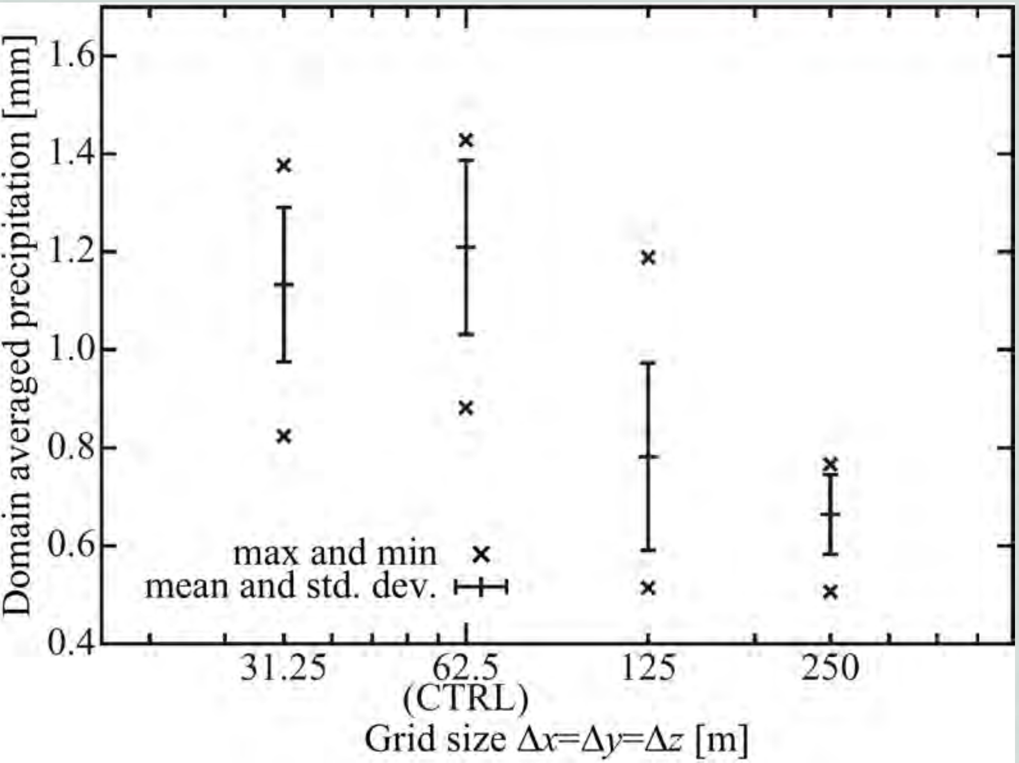

Max amount of each hydrometeor during the period

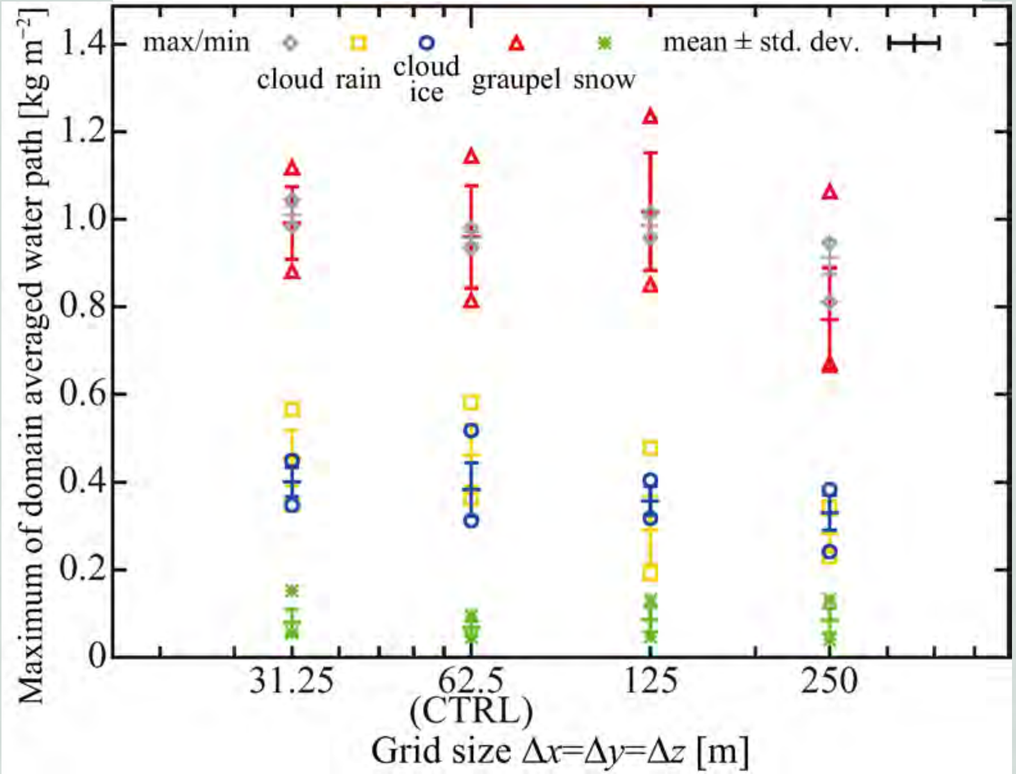

Figs. 10 and 11 of SS et al. (2020)

$\Delta x = \Delta y = \Delta z = 62.5$m seems to be sufficient.

Could be improved if we use SGS models for dynamics and microphysics.

Time step convergence

Precipitation amount

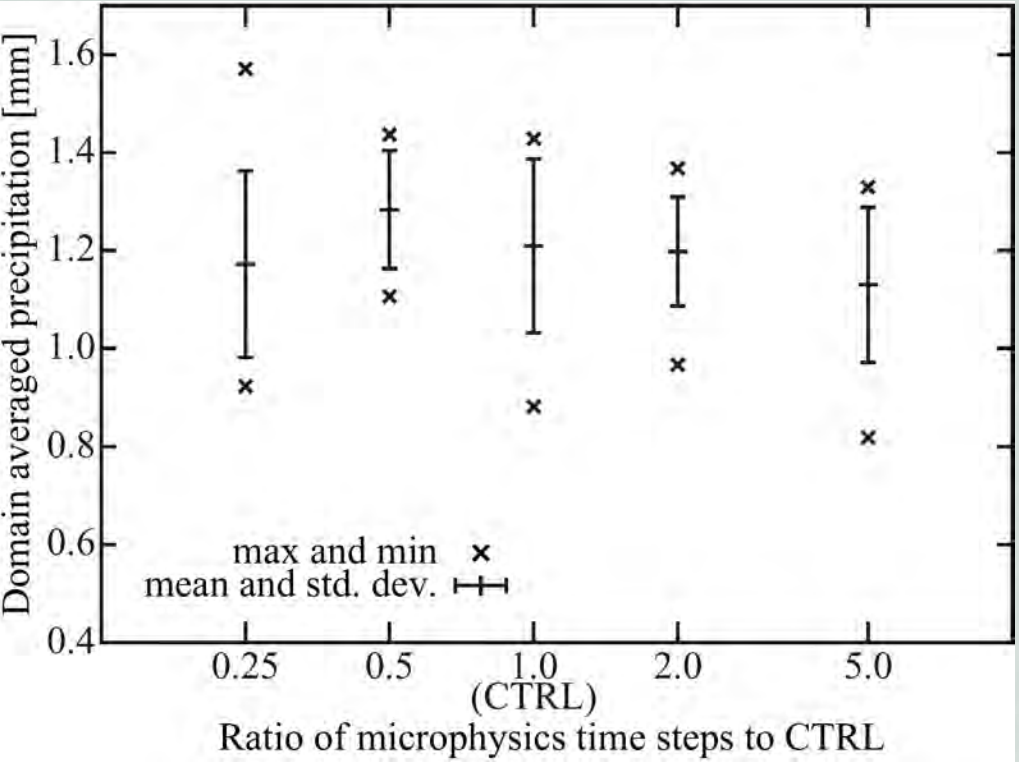

Max amount of each hydrometeor during the period

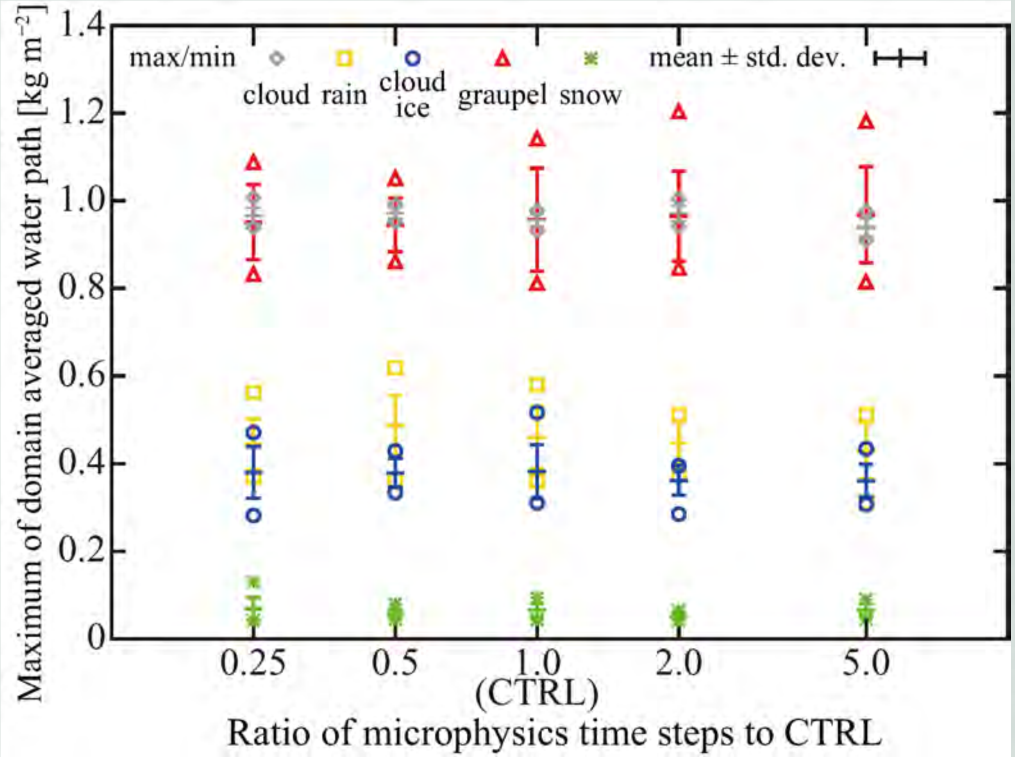

Figs. 13 and 14 of SS et al. (2020)

DTx10 diverged due to numerical instability.

Even DTx5 would be sufficient, i.e., $(\Delta t, \Delta t_{adv}, \Delta t_{fz/mlt}, \Delta t_{collis}, \Delta t_{cnd/evp}, \Delta t_{dep/sbl}, \Delta t_{dyn})$=(2.0s, 2.0s, 2.0s, 1.0s, 0.5s, 0.5s, 0.05s).

9. Possible Sophistication of the Model

Please see Sec. 9.3 of SS et al. (2020)

Ice nucleation pathways

Onset of melting

Partially frozen/melted particles

Condensation and evaporation

Deposition and sublimation

Coalescence

Riming

Aggregation

Spontaneous/collisional breakup

Subgrid-scale turbulence

Conclusions

- SDM was applied to mixed-phase clouds
- Multicomponent bin model of Chen and Lamb (1994) is translated into the particle-based framework. Latest advances in ice phase cloud microphysics are incorporated.
- 2D LES of a cumulonimbus for performance evaluation
- Life cycle of a cumulonimbus was successfully reproduced
- Mass- and velocity-dimension relationships show a reasonable agreement with existing formulas
- Numerical convergence was achieved at 128 SPs/cell
- **Our initial evaluation strongly supports the efficacy of particle-based modeling methodology**
- **The model still has a lot of room for improvement**

Take away messages

SDM and other particles-based models can connect aerosol to cloud scale seamlessly from the process level

More collaboration among lab experiments, field measurement, and cloud modeling is encouraged.

1nm ~ 10μm | 1μm ~ 1mm | 1mm ~ 1cm | 10cm ~ 10m | ~ 100m | ~ 10km | ~ 100km

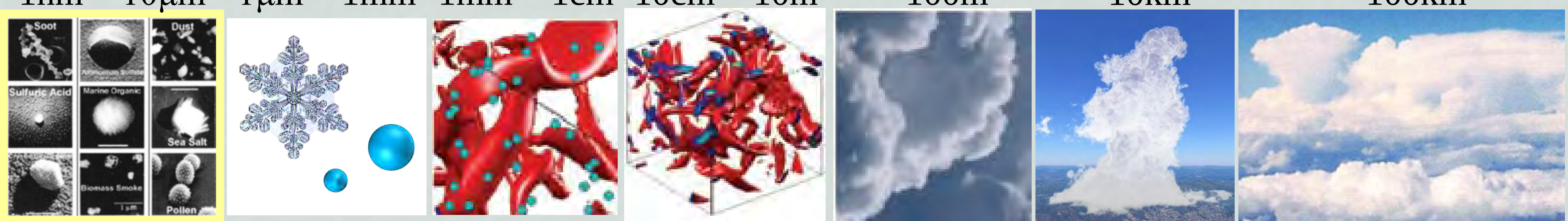

aerosol (Heintzenberg et al., 2003) | hydrometeors (SnowCrystals.com) | dissipation | cloud turbulence | entrainment | cloud | organized convection

(Fig.1 of Grabowski and Wang (2013) with modification)

(created by Matsushima)

(荒木健太郎, 2018: 世界でいちばん素敵な雲の教室より)

A. General framework of the SDM

We review the general framework of the SDM.

Introducing it in 2 steps should be helpful:

1) Conceptual model describing the dynamics of SPs

2) Numerical scheme to solve the dynamics of SPs

Dynamics of real particles

Individual dynamics $\frac{d\boldsymbol{x}_i}{dt} = \boldsymbol{v}_i, \quad \frac{d\boldsymbol{a}_i}{dt} = \boldsymbol{f}(\boldsymbol{a}_i; \boldsymbol{G}_i), \quad i \in I_{\mathrm{r}}(t).$

Stochastic coalescence, riming, and aggregation

$$\begin{aligned} P_{jk} &= K(\boldsymbol{a}_j, \boldsymbol{a}_k; \boldsymbol{G})\frac{dt}{\Delta V}, \\ &= \text{probability that particles } j \text{ and } k \text{ inside a small region} \\ &\quad \Delta V \text{ will collide and coalesce/rime/aggregate} \\ &\quad \text{in a short time interval } (t, t+dt). \end{aligned}$$

A.1. Dynamics of SPs

Individual Dynamics

We consider that SPs obey the same ODEs as RPs

$$\frac{d\boldsymbol{x}_i}{dt} = \boldsymbol{v}_i, \quad \frac{d\boldsymbol{a}_i}{dt} = \boldsymbol{f}(\boldsymbol{a}_i; \boldsymbol{G}_i), \quad i \in I_{\mathrm{s}}(t).$$

Stochastic coalescence/riming/aggregation

We consider that the coalescence/riming/aggregation of SPs is also a stochastic event, and there exists

$$P^{\mathrm{s}}_{jk} = \text{probability that super-particles } j \text{ and } k \text{ inside a small region } \Delta V \text{ will coalesce/rime/aggregate in a short time interval } (t, t+dt).$$

Requiring that SP # won't decrease after coalescence, and that the expected results is consistent with RPs, we can derive P_{jk}^{s} (Detail follows)

Definition of how a pair of SP coalesce/rime/aggregate

Let ξ_j and ξ_k be the multiplicity of the two SPs

Consider that $\min(\xi_j,\xi_k)$ pairs of real-particles contribute to the coalescence

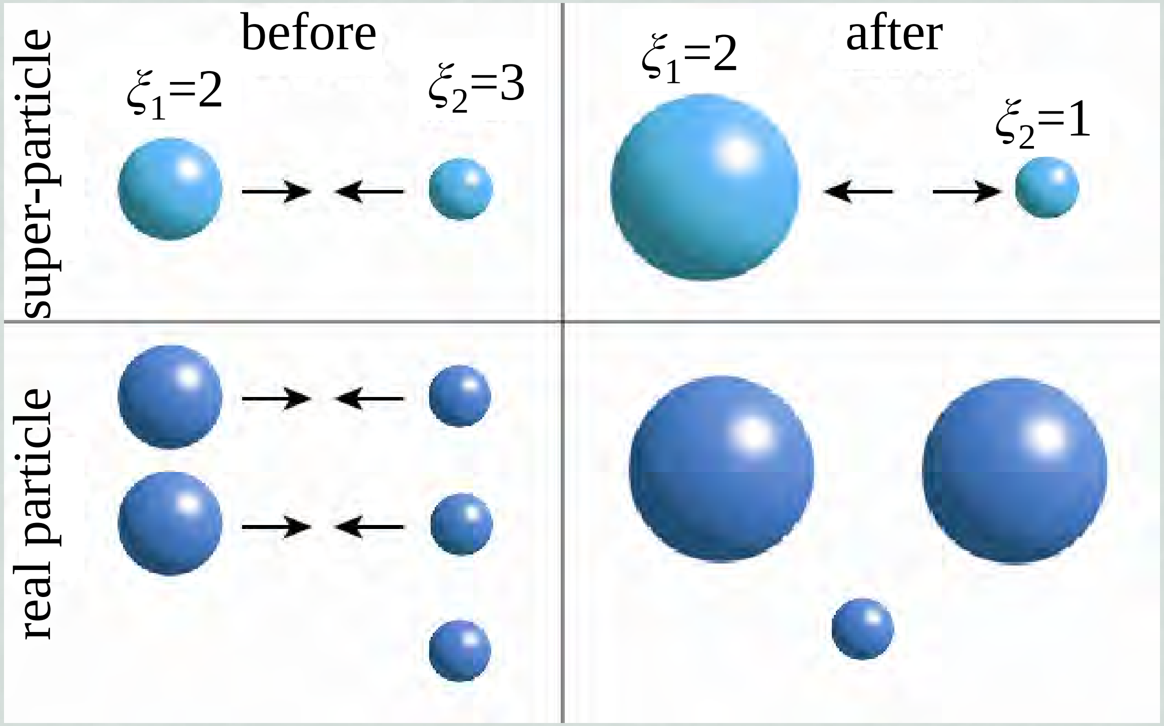

When $\xi_j=\xi_k$ we split the remaining SP

SP # is almost always conserved though RP # decreases

We now adjust the probability to get a consistent results

Definition of the coalescence probability of super-particles

Requiring that the expected number of coalesced RPs becomes the same, we get

$$\boxed{P^{\mathrm{s}}_{jk} := \max(\xi_j, \xi_k) P_{jk}.}$$

Check: Consider a coalescence between ξ_j num of RP $\boldsymbol{a}_j$ and ξ_k num of RP $\boldsymbol{a}_k$. Then, the expected num of coalesced pairs is

$$E_{jk} = \xi_j \xi_k P_{jk}. \qquad \leftarrow \text{Real World}$$

Coalescence of SPs (ξ_j, $\boldsymbol{a}_j$) and (ξ_k, $\boldsymbol{a}_k$) corresponds to a coalescence of min(ξ_j, ξ_k) pairs of RP $\boldsymbol{a}_j$ and $\boldsymbol{a}_k$

Thus, the expected num of coalesced RP num in the super-particle world becomes

$$\begin{aligned} E_{jk} &= \min(\xi_j, \xi_k) P^{\mathrm{s}}_{jk} \qquad \leftarrow \text{Super-Particle World} \\ &= \min(\xi_j, \xi_k) \max(\xi_j, \xi_k) P_{jk} \\ &= \xi_j \xi_k P_{jk}. \end{aligned}$$

A.2. Numerical Scheme for the Dynamics of SP

Numerical scheme for the individual dynamics of SPs

Individual dynamics is expressed by ODEs:

$$\frac{d\boldsymbol{x}_i}{dt} = \boldsymbol{v}_i, \qquad \frac{d\boldsymbol{a}_i}{dt} = \boldsymbol{f}(\boldsymbol{a}_i; \boldsymbol{G}_i), \quad i \in I_{\mathrm{s}}(t).$$

For each super-droplet, we solve the ODEs.

Numerical Scheme for the Stochastic Coalescence of SPs

Stochastic collision-coalescence of real particles

$$P_{jk} = E_{\mathrm{coal}}(r_j, r_k)\pi(r_j + r_k)^2 |v_j^\infty - v_k^\infty| dt/\Delta V$$

Stochastic collision-coalescence of super-particles

$$P^{\mathrm{s}}_{jk} = \max(\xi_j, \xi_k) P_{jk}.$$

Numerical scheme

We developed a DSMC-like Monte Carlo scheme for the stochastic coalescence of SPs (SS et al., 2009)

1. Make a list of SPs in each cell. ($O(N_s)$ cost) (The space is divided by a grid.)

2 techniques here (Detail follows)

2. In each cell, create candidate pairs randomly
3. For each candidate pair, draw a random number and judge whether the coalescence occurs or not.

Trick A) Pair num reduction and correction to the probability

Let N_s' be the num of SPs in a cell.

Instead of checking all the pairs ${}_{N_s'}C_2$ honestly, we reduce the num of candidate pairs to $[N_s'/2]$; Making a random permutation of SP indices and paring from the front, **we create a non-overlapping pairs** ($O(N_s')$ cost)

E.g., (1,2,3,4,5,6,7) → (2,4),(3,5),(7,6),1

With this trick the cost reduces from $O(N_s'^2)$ to $O(N_s')$

In compensation, we scale up the probability of each pair

$$\boxed{p_i := P^{(s)}_{j_i k_i} \frac{N'_s(N'_s-1)}{2} \Big/ \left[\frac{N'_s}{2}\right], \quad i = 1, 2, \ldots, \left[\frac{N'_s}{2}\right].}$$

This assures the consistency of expectation value

$$E[N_{coal}] = \sum_{j=1}^{N's} \sum_{k=1}^{N's} \frac{1}{2} \min(\xi_j, \xi_k) P^{(s)}_{jk} = E\left[\sum_{i=1}^{[N's/2]} \min(\xi_{j_i}, \xi_{k_i}) p_i\right].$$

Trick B) Handling of Multiple Coalescence

Strictly speaking, p_i>1 is not allowed, but we accept it.

Let *Ran* be a (0,1) uniform random number, and

$$q = \begin{cases} \lfloor p_i \rfloor + 1 & \text{if } \; Ran < p_i - \lfloor p_i \rfloor \\ \lfloor p_i \rfloor & \text{if } \; Ran \geq p_i - \lfloor p_i \rfloor \end{cases}$$

We consider that coalescence occurs q times

E.g., p_i = 2.7, Ran = 0.3, then q=3

This makes our method robust to larger $\Delta t_{\mathrm{collis}}$

Inaccurate if two SP sizes are similar, or if multiplicity is not large enough to accept *q* times coalescence.

Time step restriction

Δt_{collis} is restricted by the mean free time of a (real) particle, i.e., the average time for a particle between two successive coalescence

Let $\bar{P}$ be the typical probability that a particle coalescence with another particle within a small time interval Δt_{collis}

$\bar{P}$ can be evaluated as

$$\overline{P} \approx N'_{\mathrm{r}}\overline{K}\Delta t_{\mathrm{collis}}/\Delta V \approx n_{\mathrm{r}}\overline{K}\Delta t_{\mathrm{collis}},$$

where N'_{r} is the number of real particles in ΔV, $\bar{K}$ is the typical value of the kernel, and n_{r} is the number concentration of real droplets.

Requiring that $\bar{P} < 1$ has to be satisfied, we obtain

$$\Delta t_{\mathrm{collis}} < 1/(n_{\mathrm{r}}\overline{K}).$$

... Time step restriction

Let $\bar{P}_s$ be the typical probability that a collision candidate super-particle pair coalescence after the pair number reduction technique is applied.

Then, we can derive

$$\overline{P_{\rm s}} \approx \overline{P}.$$

This also supports the criteria

$$\Delta t_{\rm collis} < 1/(n_{\rm r}\overline{K}).$$